A comparative study on auditory and hyoid bones of Jurassic euharamiyidans and contrasting evidence for mammalian middle ear evolution

Jin Meng,[1,2] (iD) Fangyuan Mao,[1,3,4] Gang Han,[5,6] Xiao-Ting Zheng,[7,8] Xiao-Li Wang[7,8] and Yuanqing Wang[3,4]

[1]*Division of Paleontology, American Museum of Natural History, New York, NY, USA*
[2]*Earth and Environmental Sciences, Graduate Center, City University of New York, New York, NY, USA*
[3]*Key Laboratory of Vertebrate Evolution and Human Origins of Chinese Academy of Sciences, Institute of Vertebrate Paleontology and Paleoanthropology, Chinese Academy of Sciences, Beijing, China*
[4]*CAS Center for Excellence in Life and Paleoenvironment, Beijing, China*
[5]*Paleontology Center, Bohai University, Jinzhou, China*
[6]*Hainan Tropical Ocean University, Sanya, China*
[7]*Institute of Geology and Paleontology, Linyi University, Linyi, China*
[8]*Shandong Tianyu Museum of Nature, Pingyi, China*

Abstract

The holotypes of euharamiyidan *Arboroharamiya allinhopsoni* and *Arboroharamiya jenkinsi* preserve the auditory and hyoid bones, respectively. With additional structures revealed by micro-computerized tomography (CT) and X-ray micro-computed laminography (CL), we provide a detailed description of these minuscule bones. The stapes in the two species of *Arboroharamiya* are similar in having a strong process for insertion of the stapedius muscle. The incus is similar in having an almond-shaped body and a slim short process, in addition to a robust stapedial process with a short lenticular process preserved in *A. allinhopsoni*. The plate-like ectotympanic in the two species of *Arboroharamiya* is similar and comparable to that of *Qishou jizantang*. The surangular in the two species has a fan-shaped body and a needle-shaped anterior process. The malleus, ectotympanic, and surangular are fully detached from the dentary and should have functioned exclusively for hearing. All the auditory bones of *Arboroharamiya* display unique features unknown in other mammaliaforms. Moreover, hyoid elements are found in the two species of *Arboroharamiya* and co-exist with the five auditory bones in the holotype of *A. allinhopsoni*. The element interpreted as the stylohyal is similar to the bone identified as the ectotympanic in *Vilevolodon*. We reconstruct the auditory apparatus of *Arboroharamiya* and compare it with that of *Vilevolodon* as well as those in extant mammals and basal mammaliaforms. The comparison shows diverse morphological patterns of the auditory region in mammaliaforms. In particular, those of *Vilevolodon* and *Arboroharamiya* differ significantly: the former has a mandibular middle ear, whereas the latter possesses a definitive mammalian middle ear. It is puzzling that the two sympatric and dentally similar taxa have such different auditory apparatuses. In light of the available evidence, we argue that the mandibular middle ear reconstructed in *Vilevolodon* encounters many problems, and the so-called ectotympanic in *Vilevolodon* may be interpreted as a stylohyal; thus, the dilemma can be resolved.

Key words: auditory apparatus; ectotympanic; evolution; hearing; homology; incus; malleus; stapes; stylohyal; surangular.

Introduction

Homologies of the mammalian middle ear bones with their precursors, which are associated with the jaw joint for mastication, have long been demonstrated by developmental anatomists (Reichert, 1837; Gaupp, 1913; Goodrich, 1930; McClain, 1939). Transference of the jaw joint bones to the basicranial region as strictly auditory ossicles has attracted much attention of research in paleontology and developmental vertebrate zoology, as reviewed by Takechi & Kuratani (2010) and Maier & Ruf (2016). Recent discoveries that contributed to our knowledge on the evolution of the mammalian middle ear include discoveries of the ossified Meckel's cartilage and middle ear elements in various Mesozoic mammals (Wang et al. 2001; Meng et al. 2003; Ji et al. 2009; Luo et al. 2007a,b; Meng et al. 2011, 2018; Meng & Hou, 2016; Schultz et al. 2018). These discoveries have narrowed the morphological gap between the mandibular middle ear represented by morganucodontids (Kermack et al. 1973, 1981) and the definitive mammalian middle ear present in mammals (Allin, 1975; Allin & Hopson, 1992).

The discoveries of the auditory apparatus in the 'haramiyidan' *Vilevolodon* (Luo et al. 2017) and *Arboroharamiya* (Meng et al. 2018; Han et al. 2017) have extended our knowledge of the mammalian middle ear to 'haramiyidans', an ancient but poorly known group of mammaliaforms, and revealed novel morphological structures that have enriched as well as complicated our understanding on the evolution of the mammalian middle ear. For euharamiyidan taxa that are dentally similar and coeval in the Yanliao Biota, *Vilevolodon* and *Arboroharamiya* displayed markedly different auditory apparatuses, at least according to the current interpretations (Han et al. 2017; Luo et al. 2017). *Vilevolodon*, they claim, has a mandibular middle ear (MdME) in which the mandible has a vestigial Meckel's sulcus and a reduced postdentary trough that hold the angular (ectotympanic) and Meckel's cartilage and/or prearticular (part of the malleus). In contrast, *Arboroharamiya* has a definitive mammalian middle ear (DMME, Allin & Hopson, 1992), with all postdentary bones fully detached from the dentary, functioning exclusively for hearing; thus, the mandible has neither a meckelian sulcus nor a postdentary trough. Moreover, *A. allinhopsoni* possesses a separate surangular bone in the auditory apparatus, an element unknown in an adult individual of any other mammaliaforms. Among several uncertainties, the fundamental question is: how could the MdME and DMME coexist in taxa that are similar in dental and skeletal morphologies and that lived sympatrically in the Jurassic forest?

Evidence should prevail over interpretations in searching for any conclusion on the seemingly complicated phenomena presented in recent studies on 'haramiyidans'. Here we provide a follow-up study on the auditory apparatus of *Arboroharamiya allinhopsoni*, with focus on a detailed description of the auditory bones. We also provide descriptions on additional specimens of auditory bones from *Arboroharamiya jenkinsi* (Zheng et al. 2013) and *Qishou jizantang* (Mao & Meng, 2019a). Along with the auditory bones, we report the hyoid elements in euharamiyidans, which are critical for interpreting the auditory bones in these species. With the specimens described, we compare the morphologies of auditory bones within 'haramiyidans', and between them and other mammaliaforms. We present alternative interpretations related to the hyoid elements and their bearing on the identification of auditory bones, with focus on the ectotympanic, and present our preferred interpretation.

Materials and methods

Specimens

The primary specimens used for this study are the holotype specimen of *A. allinhopsoni* (Han et al. 2017; HG-M017, the Paleontology Center, Bohai University, Jinzhou, Liaoning Province, China), the holotype of *A. jenkinsi* (Zheng et al. 2013; STM33-9, Tianyu Museum of Nature, Shandong Province, China), and the holotype of *Q. jizantang* (Mao & Meng, 2019a; JZT-D061, the Jizantang Paleontological Museum, Chaoyang County, Liaoning Province, China). Additional data are collected from the holotype of *Xianshou linglong* (Bi et al. 2014; IVPP V16707, Institute of Vertebrate Paleontology and Paleoanthropology, Chinese Academy of Sciences, Beijing, China). The holotype of *A. allinhopsoni* (HG-M017) and *Q. jizantang* (JZT-D061) have been needle-prepared to show the ventral side of the basicranial region and preserved auditory bones. For JZT-D06, the slab containing the skull has been separated from the larger slab containing the skeleton along a natural fracture, and the lower jaw has been prepared out of the matrix.

Imaging

To obtain internal structures of exposed bones and those embedded in matrix, X-ray micro-computerized tomography (CT) and X-ray micro-computed laminography (CL) were carried out. Small specimens can be CT-scanned; these include the skull and lower jaw of *Q. jizantang* (JZT-D061). CT-scan images are of sufficient resolution for 3D rendering of the structures. Specimens preserved in slabs were scanned using a CL scanner. The resolution of CL-scan images is not sufficient for 3D rendering, but 2D images are still informative.

HG-M017 and STM33-9, both slabs, were scanned using the CL scanner at the Institute of Vertebrate Paleontology and Paleoanthropology (IVPP). The settings of the scan include a beam energy of 70–100 kV and a flux of 50–80 μA at a resolution of 26.56 μm per pixel for the skull, 7.49 μm per pixel for the auditory ossicles of HG-M017, 74.03 μm per pixel for the skeleton of HG-M017, 28.46 μm per pixel for the auditory ossicles and hyoid bones of HG-M017, 9.87 μm per pixel for the surangular of HG-M017, 10.89 μm per pixel for the ectotympanic of HG-M017, 6.34 μm and 5.78 μm per pixel for the stapes and incus of STM33-9, 28.6 μm per pixel for the skull of STM33-9, and 7.84 μm per pixel for the auditory area of JZT-D061, using a 360° rotation with a step size of 1°, resulting in a

total of 360 image slices. The resulting image slices, each with a size of 2048 × 2048 pixels, were reconstructed using a modified Feldkamp algorithm developed by the Institute of High Energy Physics, Chinese Academy of Sciences (CAS).

We CT-scanned specimen JZT-D061 using the 225 kV micro-CT at IVPP. The scan settings include a beam energy of 120 kV and a flux of 120 μA at a resolution of 28.46 μm per pixel for the skull; these were done using a 360° rotation with a step size of 0.5° and an unfiltered alini reflection target. A total of 720 transmission images were reconstructed in a 2048 × 2048 matrix of 1536 slices using a two-dimensional reconstruction software developed by the Institute of High Energy Physics, CAS. The CT scan of the auditory area of JZT-D061 was done at the micro-CT lab of the Nanjing Institute of Geology and Palaeontology (NIGPAS), using a CCD-based 3D X-ray microscope (3D-XRM) and Zeiss Xradia 520 versa. Depending on the size of the fossil specimen, a CCD-based 0.4× objective was used, providing isotropic voxel sizes of 14.79 μm with the help of geometric magnification. During the scan, the running voltage for the X-ray source was set at 70 kV, and a thin filter (LE2) was used to avoid beam-hardening artifacts. To get a high signal-to-noise ratio, projections over 360° were collected for the skull (JZT-D061) and the exposure time for each projection was set as 3 s.

We took optical images using a Canon digital camera with a macro lens and a Zeiss microscope (SteREO Discovery v.20) with a digital imaging system (AxioVision SE64 Rel. 4.9). All facilities we used for the study (except Zeiss Xradia 520) are installed in the Key Laboratory of Evolutionary Systematics of Vertebrates, Institute of Vertebrate Paleontology and Paleoanthropology (IVPP), CAS.

Measurements of the teeth and small postcranial elements (lengths and angles) were taken using the AxioVision SE64 Rel. 4.9 software on a Zeiss microscope (SteREO Discovery v.20) and rechecked with enlarged photographs of the specimen with scales, using ImageJ 1.49v.

Terminology

In this study, we use 'auditory bones' to imply the stapes, incus, malleus, ectotympanic, and surangular that are present in *Arboroharamiya*. We restrict 'middle ear bones' to the first three of the five auditory bones. The auditory bones and the middle ear bones are used interchangeably for the stapes, incus, and malleus.

Results

Arboroharamiya allinhopsoni

Both optic and CL images show that the teeth are in occlusal positions (Figs 1 and 2). The association of the left auditory bones is well-preserved, the bone nearly in their anatomical positions. A total of five bones are identified as the stapes, incus, malleus, ectotympanic, and surangular. Each bone is nearly complete with its ventral (or ventrolateral) side exposed. The promontorium and occipital condyle on both sides of the cranium are preserved in good condition; their relative positions show that the crushed skull was slightly skewed. The preserved structures collectively show that alteration of the auditory bones is minor. Measurements of the auditory bones are presented in Fig. 3.

Stapes

The stapes is bicrurate and has a distinct posterior process on the posterior crus (Figs 1–3). Its footplate plugs the fenestra vestibuli, more or less in its anatomical position. The footplate is oval-shaped, similar to but smaller than the fenestra vestibuli; the latter measures 1.1 mm in length and 0.51 mm in width. The size difference suggests that the footplate was probably connected to the rim of the fenestra vestibuli by an annular ligament in life, which allowed vibrations of the stapedial footplate at the fenestra vestibuli. The peripheral edge of the footplate is thick and the central portion is thin, so that the lateral side of the footplate is concave. CL images reveal a small canal within the bone that circles within the thick periphery of the footplate, as in *A. jenkinsi* (Fig. 4E,H). The footplate is not as distinct as that in extant mammals because its edge aligns with the external edges of the crura. The anterior and posterior crura are rod-like, with the posterior one being thicker. The crura arch outward and between them is a large oval stapedial foramen. Coupled with the distinct transverse groove on the promontorium, this infers that there was a sizable stapedial artery that went through the foramen in life. At the lateral end, the stapes has a head that is narrower than the footplate but matches the size of the lenticular process of the incus. The posterior crus has a strong posterior process, interpreted as for insertion of the stapedius muscle (PISM, Meng & Hou, 2016; Meng et al. 2018). The process is rod-like and slightly curved; it extends to the stapedius fossa. The posterior end of the process is slightly inflated (Figs 1B, 2B, and 3).

Incus

The incus is lateral to the stapes and articulates with the head of the stapes by the lenticular process (Figs 1 and 2B). This articulation indicates that the two ossicles are more or less in their anatomical positions, an unusual preservation of the middle ear bones in early mammals. The body of the incus is situated in a concavity that is identified as the epitympanic recess. From the relationship of the recess with the glenoid fossa, the lateral wall of the epitympanic recess is probably formed by the squamosal. The ventral surface of the body is almond-shaped and smoothly convex, most probably for articulation with the malleus and reminiscent of the articular-quadrate jaw joint in non-mammalian cynodonts (Allin, 1975; Kemp, 2007). The stapedial process (long crus) is clearly delimited from the body and extends anteromedially. The process is robust compared with that in extant therians, and tapers anteriorly. Its distal end turns medially to form the lenticular process that articulates with the head of the stapes. The neck of the lenticular process is short, and the width of the lenticular process matches the width of the head of the stapes.

CL images show that there is a 'network' within the incus, which we tentatively term the incus network (Fig. 4A–C). This feature is nearly identical to that of *A. jenkinsi*

Fig. 1 Skull and auditory bones of *Arboroharamiya allinhopsoni* (holotype, HG-M017). (A) The skull in ventral view (roughly). (B) Close-up view of the auditory bones, corresponding to the boxed area with dashed black line in (A). The arrows in (A) and (B) point to the posterior tuberosity of the alisphenoid (comparable to that of *Qishou* in Fig. 8). (C) Stereopairs of the basicranial region with focus on the auditory bones. The boxed area with dashed white line corresponds to the area in Figs 2A and 5A–C (note its position relative to the angular process and the auditory bones). agp, angular process; apm, anterior process of the malleus (prearticular); asa, anterior process of the surangular; cop, coronoid process; cv1, first cervical vertebra; cv2, second cervical vertebra; cvp, circumopromontorial venous plexus; exo, exoccipital; fi, fossa incudis (in epitympanic recess); fv, fenestra vestibuli; gf, glenoid fossa; hst, head of the stapes; hy, hyoid element (ceratohyal or epihyal); ic, incus; ju, jugal; loc, left occipital condyle; lp, lenticular process of the incus; lP3, left third upper premolar; mal, malleus; mc, mandibular condyle; mf, mental foramen; mm, manubrium of the malleus; mp, medial process of the malleus; pf, perilymphatic foramen; pic, stapedial process of the incus; pips, passage for the interior petrosal sinus; pm, promontorium; ppr, paroccipital process; ptp, post-tympanic process of the squamosal; rdi, right lower deciduous incisor; rdl2, right second upper deciduous incisor; rM1, right first upper molar; roc, right occipital condyle; rP3, right third upper premolar; rp4, right fourth lower premolar; rP4, right fourth upper premolar; rtm, ridge for attachment of the anterior part of the tympanic membrane; sa, surangular; sf, stapedius fossa; spg, groove for the stapedial artery; st, stapes; tldi, tip of left lower deciduous incisor; ty, ectotympanic; ty-d, lateral ectotympanic part presumably equivalent to the dorsal part of the angular; ty-r, medial ectotympanic part presumably equivalent to the reflected lamina. za, zygomatic arch.

(Fig. 4D–H). The incus network has a central loop, which gives rise to a branch that extends into the short process (crus). The nature of this network is unknown; it is best interpreted as dense bone, in contrast to the rest of the incus, which consists of spongy bone or even hollowed spaces. This dense bony structure may be a central framework that helps to increase the rigidity of the incus, given that the incus functions as the centerpiece of the leverage system for transmitting sound vibrations in the middle ear. Alternatively, but less likely, the structure may represent a sinus network that is filled by dense mineral during preservation.
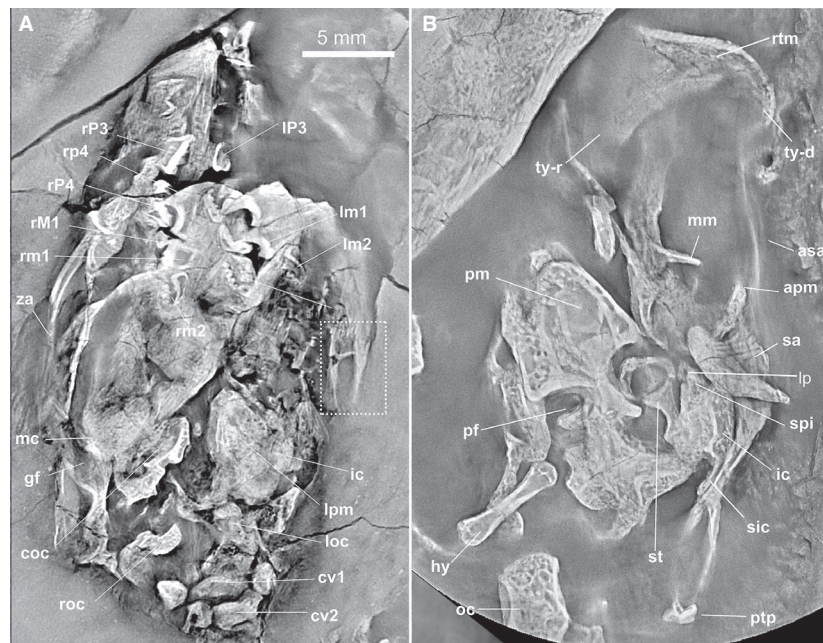
Fig. 2 CL images of the skull and auditory bones of *Arboroharamiya allinhopsoni* (holotype, HG-M017). (A) The skull in ventral view (roughly). (B) Close-up view of the auditory bones, corresponding to the boxed area with dashed black line in Fig. 1A. The boxed area with dashed white line corresponds to the area in Figs 1A and 5A–C. apm, anterior process of the malleus (prearticular); asa, anterior process of the surangular; coc, cochlear canal; cv1, first cervical vertebra; cv2, second cervical vertebra; fv, fenestra vestibuli; gf, glenoid fossa; hy, hyoid element (ceratohyal or epihyal); ic, incus; ldl2, left second upper deciduous incisor; lm1, left first lower molar; lm2, left second lower molar; loc, left occipital condyle; lp, lenticular process; lP3, left third upper premolar; lp4, left lower forth premolar; lpm, left promontorium; mc, mandibular condyle; mm, manubrium of the malleus; pf, perilymphatic foramen; pic, stapedial process of the incus; pm, promontorium; ptp, post-tympanic process of the squamosal; rM1, right first upper molar; rm1, right first lower molar; rm2, right second lower molar; roc, right occipital condyle; rP3, right third upper premolar; rp4, right fourth lower premolar; rP4, right fourth upper premolar; rtm, ridge for attachment of the anterior part of the tympanic membrane; sa, surangular; sic, short process of the incus; spi, stapedial process of the incus; st, stapes; ty-d, lateral ectotympanic part presumably equivalent to the dorsal part of the angular; ty-r, medial ectotympanic part presumably equivalent to the reflected lamina. za, zygomatic arch.

The short process (crus) was not identified in the original study (Han et al. 2017) because it is difficult to see under a microscope or from the optic image (Fig. 1). Comparing CL images with those of the incus of *A. jenkinsi*, we find that the incus of *A. allinhopsoni* has a slim short process, as in *A. jenkinsi* (Meng et al. 2018; Figs 3 and 4). The short process is lodged in a narrow trench posterior to the epitympanic recess; it probably helped to anchor the incus to the cranial region, as in the ear of extant mammals (Doran, 1878; Segall, 1970; Henson, 1974; Fleischer, 1978), although the shape of the short process in *A. allinhopsoni* is unique.

Malleus
The malleus is preserved dorsal to the surangular and ectotympanic, which implies that if these bones were placed vertically, the malleus would be medial to the surangular and the ectotympanic, similar to the relationship of the postdentary bones in the mandibular middle ear, for instance, of *Morganucodon* (Kermack et al. 1981). The posterior portion of the malleus is plate-like. This part is interpreted as the transverse part of the malleus, as in *Ornithorhynchus* (Zeller, 1989, 1993). The bone must be slightly displaced anteriorly such that its posterior edge is in contact with the

articulation of the incus and stapes; this is not a normal or functional position. It is most likely that the incudal facet of the malleus is on the dorsal side of the transversal part so that the transverse part of the malleus articulated with the ventral surface of the incudal body in life.

The transverse part is not a flat plate; instead, it is concave ventrally and delimited posteriorly by a curved ridge. Its lateral edge extends anteriorly as the anterior process of the malleus, which is partly exposed by preparation, but its anterior part is still in the matrix. The CL-image shows that the anterior process extends to the point where the lateral process of the ectotympanic ends posteriorly or the area where the anterior process of the surangular shows a breakage (Fig. 2B). The anterior process of the malleus is proportionally short compared with those in monotremes and many therians (Doran, 1878; Segall, 1970; Henson, 1974; Fleischer, 1978); it adjoins the anterior process of the surangular.

At the anteromedial end of the transverse part, there is a bony prong that projects laterally; this prong is identified as the manubrium. As shown in the optic and CL images (Figs 1B and 2B), the prong is thick at its base and tapers toward the tip. The distal portion of the manubrium is
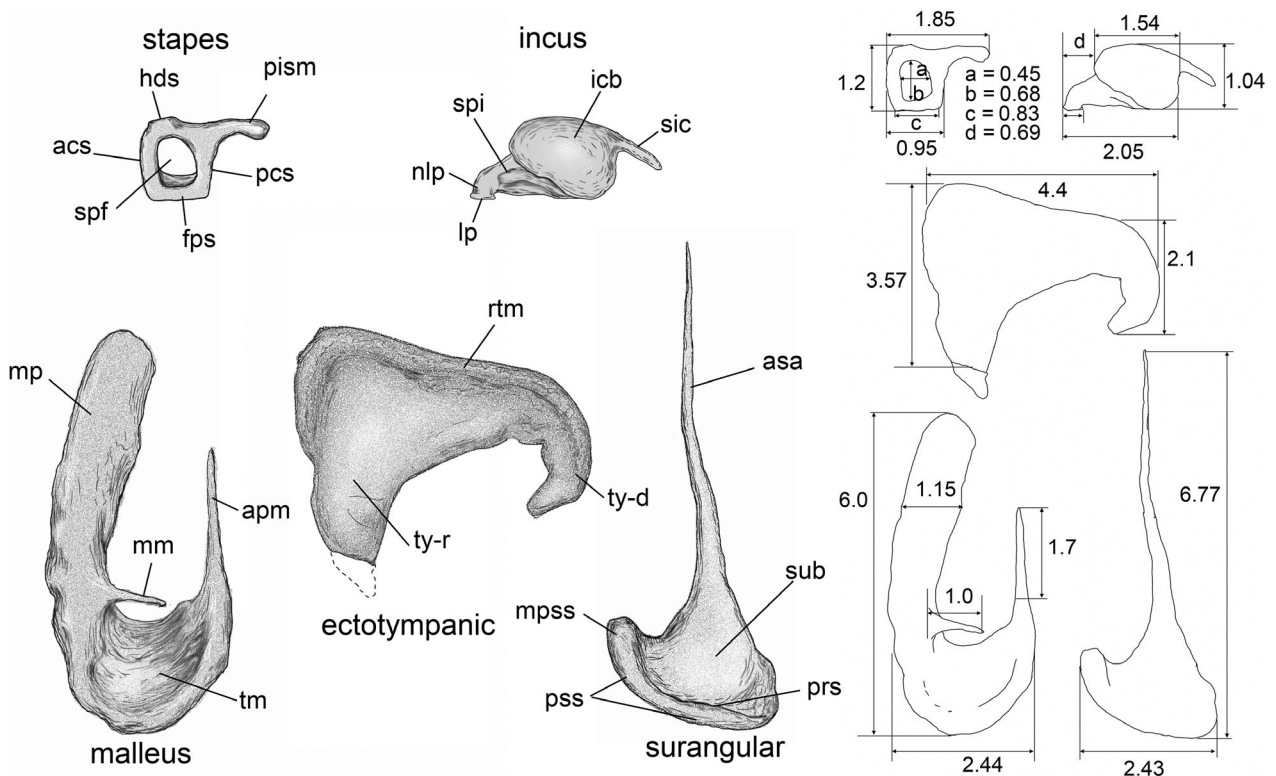
Fig. 3 Drawings and measurements of the left auditory bones of *Arboroharamiya allinhopsoni*. Measurements are in millimeters (mm). acs, anterior crus of the stapes; apm, anterior process of the malleus (=prearticular); asa, anterior process of the surangular; fps, footpate of the stapes; hds, head of the stapes; icb, body of the incus; lp, lenticular process; mm, manubrium of the malleus; mp, medial process of the malleus; mpss, medial portion of the posterior surface of the surangular; nlp, neck of the lenticular process; pcs, posterior crus of the stapes; pism, process for insertion of the stapedius muscle of the stapes; prs, posterior ridge of the surangular; pss, posterior surface of the surangular; rtm, ridge for attachment of the anterior part of the tympanic membrane; sab, body of surangular; sic, short process of the incus; spf, stapedial foramen of the stapes; spi, stapedial process of the incus; sub, body of the surangular; tm, transverse part of the malleus; ty-d, lateral ectotympanic part presumably equivalent to the dorsal part of the angular; ty-r, ectotympanic part presumably equivalent to the reflected lamina.

slightly ventral to the plane in which the rest of the malleus sits. Anterior to the manubrium is the robust medial process, a feature unknown in the malleus of mammals. This process has been homologized to the retroarticular process of the articular (Han et al. 2017). If this interpretation is correct, the elongate medial process is unique in *Arboroharamiya*. In ventral view, the edges of the medial process are slightly curved, convex medially and concave laterally. It is dorsoventrally thick at the base, and gradually thins and slightly widens anteriorly. The ventral surface of the medial process is slightly convex and smooth. The anterior tip of the medial process is dorsal to the ectotympanic.

In regard to the morphology of the malleus in *A. allinhopsoni*, an alternative interpretation was provided by Dr. Edgar Allin (personal communication in an email to J.M., 26 November 2017): "Full separation of the auditory elements from the mandible is clear in *A. allinhopsoni*, as is persistence of the surangular! However, there are puzzles posed by its ossicular morphology. I would interpret certain features differently than the authors do. In particular I think that the 'medial process' of the malleus is actually the manubrium, given its orientation parallel to the anterior process as in many existing mammals, however large and flat it is. I'd consider it to be a neomorphic outgrowth of the retroarticular process (conceivably of hyoid arch origin). The peculiar prong identified as the manubrium seems too different in orientation and may perhaps have served as a modified insertion of a tensor tympani muscle. The overlapping of the actual manubrium and ectotympanic as illustrated seems improbable and may be the result of postmortem displacement of the latter, correctable by rotation". The parallel orientation of the manubrium and the anterior process is indeed common in extant mammals (Wible, 2008; Wible & Spaulding, 2012), but variation exists (Doran, 1878; Segall, 1970; Henson, 1974; Fleischer, 1978). Because the tympanic membrane forms within the region of the first pharyngeal arch (Furutera et al. 2017), the interpretation of the medial process as the manubrium in association with the tympanic membrane gains support from developmental studies. The stapes and incus of *Arboroharamiya* are unequivocal, but they differ considerably from those of known mammaliaforms; it would be
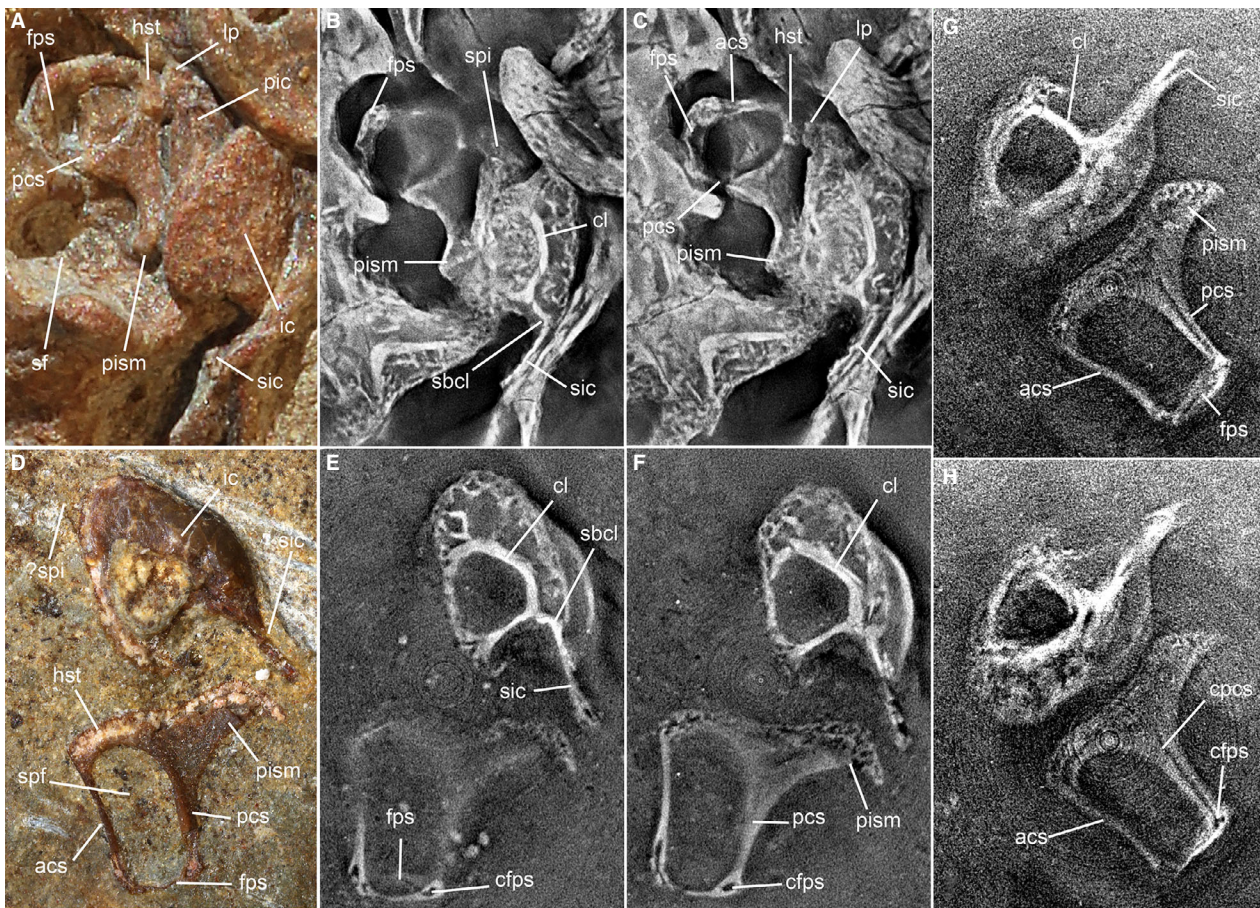
Fig. 4 Left stapes and incus of *Arboroharamiya*. (A) Ventral view of stapes and incus of *Arboroharamiya allinhopsoni* (HG-M017). (B–C) Two slices of CL images of the left stapes and incus, with the specimens with roughly the same orientation as in (A) (slightly smaller in scale). (D) Possibly ventral view of left stapes and incus of *Arboroharamiya jenkinsi* (STM33-9). (E,F) Two slices of CL images of the left exposed stapes and incus, with a slightly different orientation and scale from those in D. (G,H) Two slices of CL images of the embedded right stapes and incus. acs, anterior crus of the stapes; cfps, canal that circles within the periphery of the footplate; cl, central loop of the incus network; cpcs, canal in the posterior crus of the stapes; fps, footplate of the stapes; hst, head of the stapes; ic, incus; lp, lenticular process of the incus; pcs, posterior crus of the stapes; pism, process for insertion of the stapedius muscle; sbcl, short process branch of the central loop; sf, stapedius fossa; sic, short process of the incus; spf, stapedial foramen; spi, stapedial process of the incus (?spi in D indicates the possible base of the stapedial process).

unsurprising if the morphology of the malleus differs considerably from what we know in other mammaliaforms.

Ectotympanic

The ectotympanic is a plate-like bone, with a smooth and gently concave ventral surface. The anterolateral and anteromedial corners are rounded; there is no anterior limb at the anterolateral end of the bone. In other words, there is no structure that connects the ectotympanic to the dentary. The bone thickens along the anterior rim to form a low ridge that was interpreted as for the attachment of the anterior edge of the tympanic membrane (Han et al. 2017). As preserved, its medial portion is a broad process that extends posteriorly, and narrows and thins toward the tip. The end of the medial process was a breakage, suggesting that the tip of the process was broken. The medial process was interpreted as homologous to the reflected lamina of

the angular in non-mammalian cynodonts (Han et al. 2017), which is here reiterated. The lateral portion of the ectotympanic also extends posteriorly as a process, but it is smaller than the medial one. The posterior edge of the ectotympanic is thin, forming a well-defined curve. On the posterior area of the lateral process, the edge becomes irregular, and there is a notch and a tiny projection (Fig. 1B); whether these are natural or created by breakage cannot be determined. The width of the ectotympanic is about 18% of the mandible length (23.8 mm; Han et al. 2017).

Surangular

This is a unique element in the auditory apparatus of mammaliaforms. The reason to identify the bone as the surangular has been given by Han et al. (2017): supplementary information) and will not be repeated here. The surangular has a fan-shaped body that gradually thins anteriorly to

form a needle-shaped anterior process. The bone surface on the medial portion of the body is smooth but slightly uneven on the lateral portion. The posterior end of the body has a curved posterior outline, and along the posterior rim, the bone thickens to form a low ridge. There is also a medial process that is the dorsoventrally thickest region of the body. This posterior surface of the body is reminiscent of an articular surface, which is interpreted as the remnant surangular boss that articulated with the initial glenoid fossa of the squamosal in basal mammaliaforms. Judging from their similar shape, the dorsal side of the surangular body was most likely lodged in the concave area on the ventral side of the transversal part of the malleus in life. The posterior end of the body is a long and convex surface, and the convex surface is best shown on the medial hook-shaped process.

The anterior process has a smooth surface and, in preserved condition, extends parallel to the anterior process of the malleus, gradually tapering distally to become needle-shaped. The process is slightly curved, bowing laterally. As revealed by the CL-image, the needle-shaped anterior portion is dorsal to the ectotympanic, and there is a breakage on the process. If the bones were positioned vertically, the very tip of the surangular would be on the medial side of the ectotympanic. Although the anterior process is long, it does not pass over the anterior edge of the ectotympanic. As preserved, the malleus, the ectotympanic, and the surangular form a frame, probably for holding the tympanic membrane. It is also clear that the whole apparatus does not connect to the dentary, unless by ligaments.

Hyoid elements

A small bone that has a rod-like body with two expanded and rounded ends has been identified as a hyoid element (Han et al. 2017); it may be the ceratohyal or epihyal (Figs 1B and 2B). In addition, CL scanning reveals another bony element near the angular process of the dentary (Figs 2B and 5A–C). We tentatively identify this bone as the stylohyal and will provide discussions on its identification after a similar element in *A. jenkinsi* is described below. This element has an intriguing morphology – a rod-like body with a lateral process that branches from the main body; thus, the bone can be divided into three parts, the anterior, the posterior, and the lateral processes. Because the actual orientation of the bone in this specimen is uncertain, we use the preserved position in describing its structures. The lateral process inclines anteriorly and forms an angle about 80° with the anterior processes; its tip, however, bends posteriorly (Figs 2A and 5A–C), similar to that of *A. jenkinsi* (Fig. 5D–F). The posterior process vaguely shows a tendency to widen. These processes may be equivalent to the superior, the posterior, and the inferior rami, respectively, of the stylohyal of some mammals (Inuzuka et al. 1975; Shoshani et al. 2007).

Arboroharamiya jenkinsi

The holotype (STM33-9) of *A. jenkinsi* was preserved as the main part and the counterpart of a split slab (Zheng et al. 2013). On the main part, a set of the stapes and incus (probably from the left side) is exposed and has been reported elsewhere (Meng et al. 2018; Fig 6A). CL scanning, however, reveals additional auditory bones and hyoid elements in the matrix, including the right stapes and incus that were preserved in association (Fig. 6B). Other elements include the surangular bones, one ectotympanic, and two hyoid elements. It is an unusual condition that these minuscule elements and teeth were preserved in isolation, but the cranial bones were mostly gone. Because of the thick and large slab, it is difficult to obtain a clear image of the bones embedded in the matrix. Nonetheless, the morphology and relative sizes of these isolated bones still add useful information for their identification and interpretation.

Stapes

The two sets of the stapes and incus are comparable in morphology and size (Fig. 6a,b), but it is still difficult to identify which pair is from the right or left side of the cranium. The general morphology has been described in detail for the exposed stapes (Meng et al. 2018; Fig. 4B). CL images reveal that, similar to that of *A. allinhopsoni*, the stapedial footplate of *A. jenkinsi* is thick in its peripheral edge and thin in its center so that the lateral surface is concave. The cross-section shows a small ring-shaped canal that circles within the footplate periphery and is confluent with a medullary canal-like cavity in the posterior crus (Fig. 4E–H). In contrast, the process for insertion of the stapedius muscle (PISM) is a thin plate. The CL images confirm the original identification of the footplate and head of the stapes (Meng et al. 2014), contrary to an alternative interpretation of the bone (Schultz et al. 2018).

Incus

The identification of the isolated incus and its relationship to the stapes were uncertain when they were first reported (Meng et al. 2018). In light of the two bones preserved *in situ* in *A. allinhopsoni*, the identification of the incus in *A. jenkinsi* is confirmed. The general morphology of the exposed incus (Figs 4 and 6) has been described elsewhere (Meng et al. 2018). CL scan reveals a distinct incus network that is similar to that of *A. allinhopsoni* (Fig. 4E,F). Owing to the larger size of the bone, the incus network of *A. jenkinsi* is more clearly shown than that in *A. allinhopsoni*. It appears that the area surrounded by the central loop of the incus network is hollow in *A. jenkinsi*. The central loop gives a branch that extends into the short process; this configuration helps to orientate and identify the short process of the incus. The exposed incus shows a possible broken base of the stapedial process, but CL scan did not reveal the stapedial process in either incus.
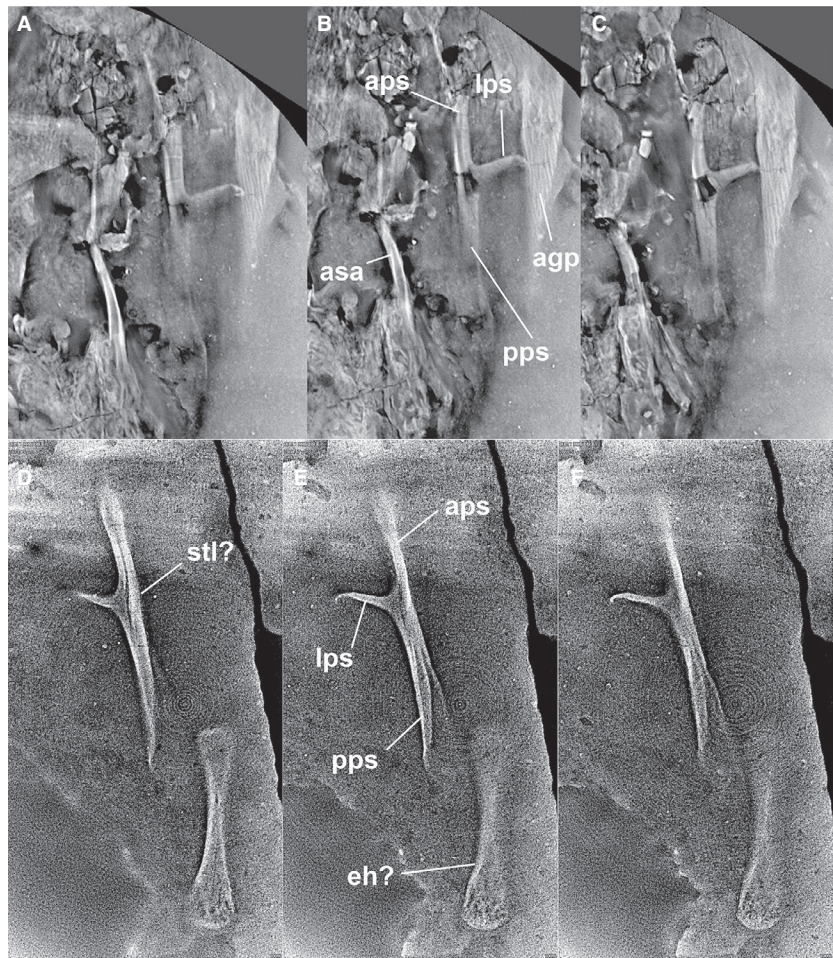
Fig. 5 Hyoid elements of *Arboroharamiya*. (A–C) CL images showing the possible stylohyal near by the angular process in *Arboroharamiya allinhopsoni* (HG-M017). (D–F) CL images showing isolated hyoid elements of *Arboroharamiya jenkinsi* (STM33-9), possibly the stylohyal and epihyal. (A–C) correspond to the boxed area with dashed white line in Figs 1A and 2A. (D–F) are preserved within the matrix (Fig. 6e). agp, angular process; aps, anterior process of the stylohyal; asa, anterior process of the surangular; eh?, epihyal (tentatively identified); lps, lateral process of the stylohyal; pps, posterior process of the stylohyal; stl?, stylohyal (tentatively identified).

Ectotympanic

An isolated ectotympanic is revealed by CL scan (Figs 6f and 7A,C). Because of the thick slab, the CL image is not very clear, but it can be seen that the general shape is similar to that of *A. allinhopsoni* (Fig. 7C,D). The bone appears complete with a smooth and slightly thickened edge; it is unlikely to be a fragment of any other cranial or postcranial bone. The end of the medial process shows a twist that may represent the contact area with the malleus (Fig. 7C). The anteromedial corner of the bone is angular. The element is estimated to be 7.1 mm wide, 6.8 mm long on the medial side, and 3 mm long on the lateral side; the width is 19% of the mandible length (37.65 mm; Meng et al. 2014), similar to that of *A. allinhopsoni*.

Surangular

Two elements are identified as possible surangular; one is preserved overlapping with the proximal end of the ulna (Fig. 6B) and the other is in isolation (Fig. 6c,g). Their identification is based on their similar shape to the surangular of *A. allinhopsoni*. It has a broad body that gradually narrows anteriorly to form a needle-like anterior process.

Hyoid elements

Two bones are tentatively identified as the epihyal and stylohyal (Figs 5D–F and 6E). The epihyal is rod-like, with rounded ends that are thicker than the middle portion of the bone. The possible stylohyal is similar to that of *A. allinhopsoni* in having a long body and a lateral process (Fig. 5D–F); it differs from the latter in that the lateral process is proportionally slim with a sharp tip that bends posteriorly. In *A. allinhopsoni* (Fig. 5A–C) the lateral process is relatively thick and its tip, also bending posteriorly, is blunt. The series of CL images reveals that the posterior process is not a solid rod; instead, it appears to bear a notch that widens posteriorly; a similar condition is vaguely shown in the stylohyal of *A. allinhopsoni*.

Qishou jizantang

Qishou jizantang (Mao & Meng, 2019a) is dentally similar to *Shenshou* (Bi et al. 2014) and *Maiopatagium* (Meng et al. 2017), although the tooth occlusal patterns are considerably different between *Qishou* and *Shenshou* on the one hand and *Maiopatagium* on the other (Mao & Meng, 2019b). Only the ectotympanic is preserved on the
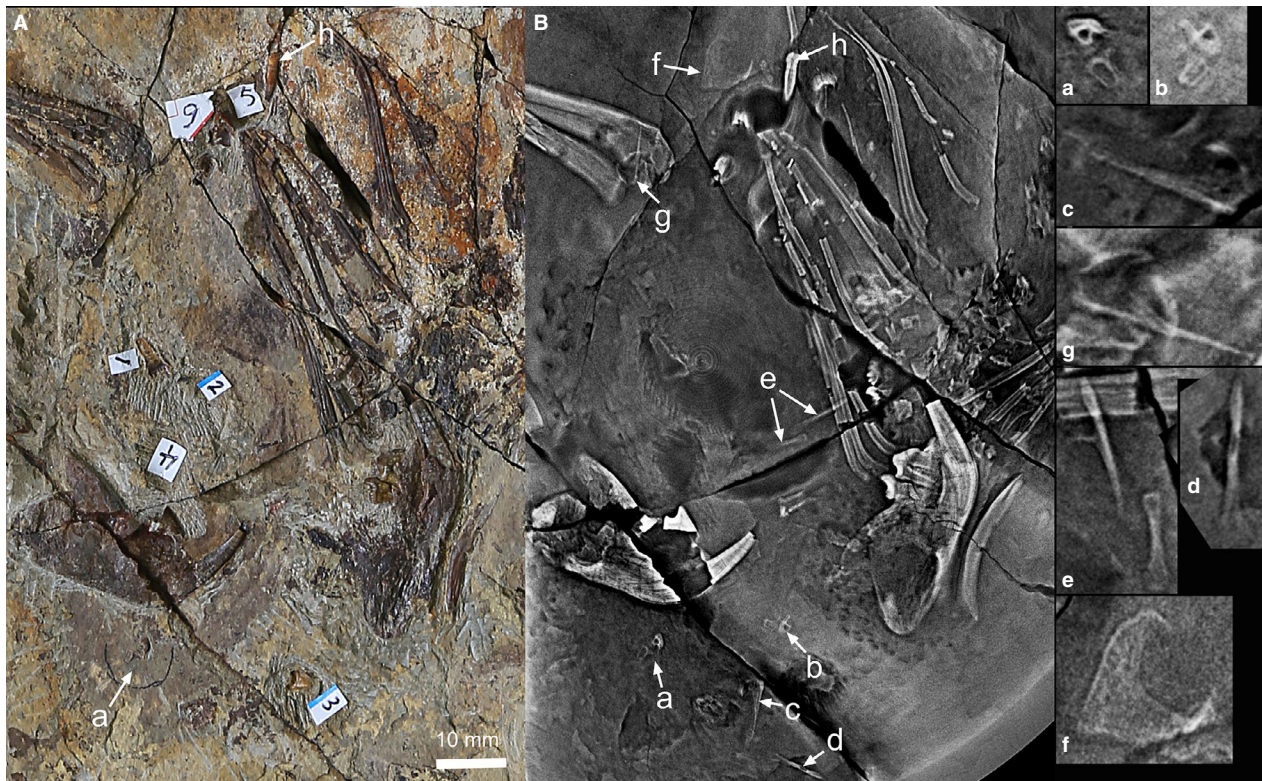
Fig. 6 Local views of the holotype (STM33-9A) of *Arboroharamiya jenkinsi* that contain the lower jaws and auditory and hyoid bones. (A) Optic image of the specimen in which the numbers mark the positions of preserved teeth, some of which have been removed for SEM imaging (Meng et al. 2014). The exposed auditory bones are the stapes and incus (a). (B) CL scan image that shows the scattered auditory and hyoid elements (note that the cranial bones are nearly absent), including the exposed stapes and incus (a), the second set of the stapes and incus (b), the surangular (c), a partial stylohyal (d), the possible stylohyal and epihyal (e), the ectotympanic (f), and the other surangular (g), and presumably an upper incisor (h). Close-up views of the corresponding elements from the same CL scan are presented in the right column. The close-up images are on the same scale so that their relative size can be accessed. Clearer images of some of these elements are presented in Figs 4E–H and 5D–F, and 7.

left side of the basicranium (Fig. 8). Except for a fracture at the medial process, the ectotympanic is complete. Here we provide a description of the basicranial region and the CT-rendered ectotympanic that shows more details of the bone. In the ventral view of the cranium of *Q. jizantang*, the choanae are marked by the curved posterior border of each palatine, and the perpendicular process of the palatine forms the lateral wall of each choana (Fig. 8). The paired pterygoid bones are thin plates and form most of the roof and vertical lateral walls of the nasopharyngeal passage posterior to the choanae. The pterygoid hamulus was broken. The general morphology of this area is therian-like, except that it is proportionally long in relation to the short dentition. Lateral to the pterygoid is the alisphenoid that forms the ventrolateral wall of the braincase; it terminates posteriorly as an irregular tuberosity. A similar tuberosity was present in the similar region in the basicranium of *A. allinhopsoni* (Fig. 1). By its position, this structure may have functioned as a supporting site for the auditory bones. The promontorium is present on each side; posterolateral to it is the epitympanic recess. Still lateral to the

epitympanic recess is the glenoid fossa. The occipital condyles, the basioccipital, and the basisphenoid are preserved in good condition. The preserved basicranial region rules out the possibility that the element identified as the ectotympanic is a different bone or a fragment of any bone, such as the pterygoid hamulus or the lateral flange in the cranium.

As in *Arboroharamiya*, the ectotympanic is plate-like and has well-defined edges and processes (Mao & Meng, 2019a; Figs 1, 2, 6, and 7). It differs from that of *Arboroharamiya* (Figs 6 and 7) in being thicker and having a stronger ridge for attachment of the anterior part of the tympanic membrane. In addition, its anterior border is narrower and curved. In contrast, the anteromedial corner of the ectotympanic of *A. jenkinsi* is more angular. The ectotympanic measures 3.4 mm wide and 2.7 mm long on the lateral side (medial side broken), which is proportionally narrower but longer than that of *Arboroharamiya*. The width of the ectotympanic is about 11% of the mandible length (30.9 mm; Mao & Meng, 2019a), proportionally smaller than that of *Arboroharamiya*.
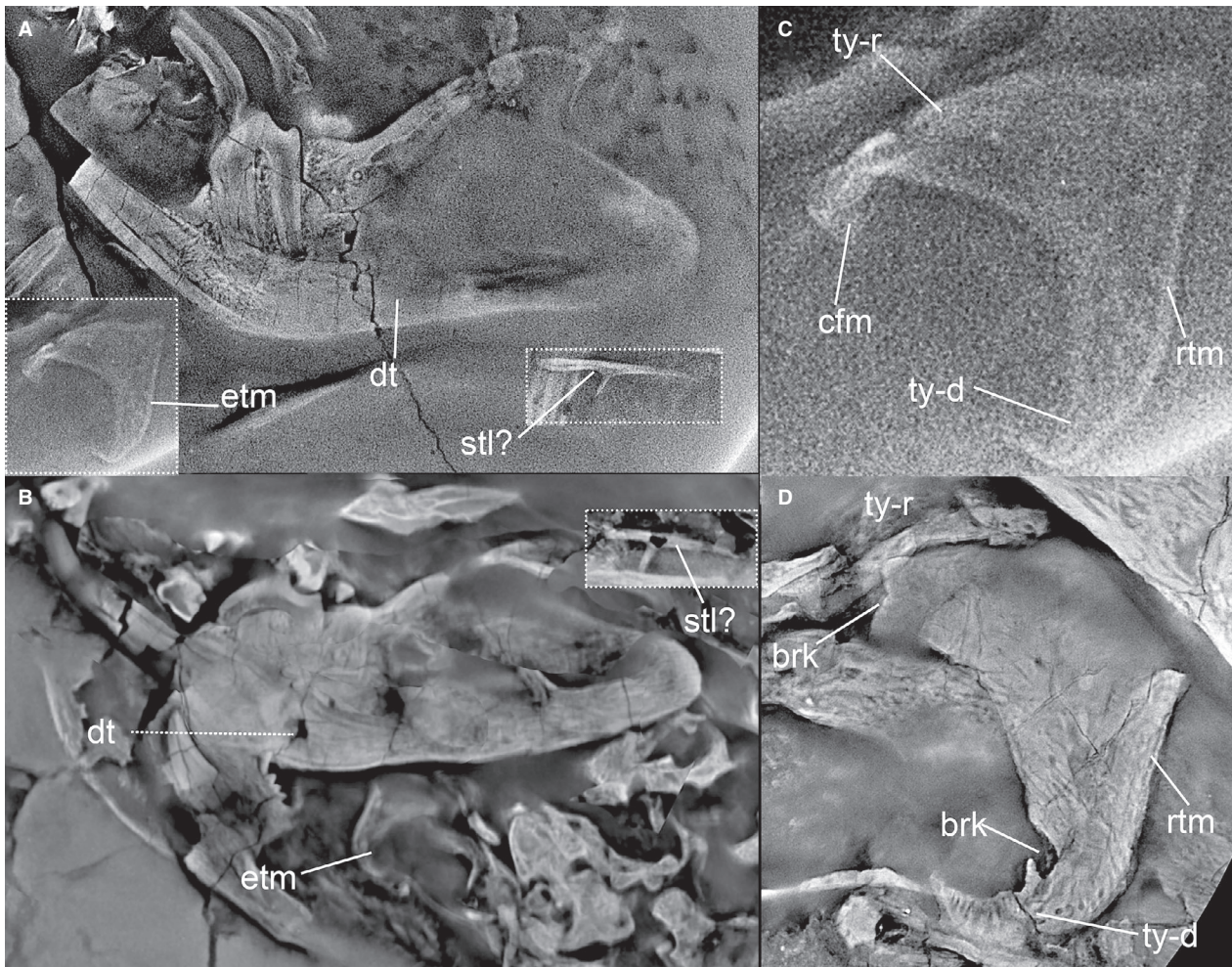
© 2019 Anatomical Society

Fig. 7 CL images comparing the relative size of the ectotympanic and possible stylohyal in *Arboroharamiya*. (A) The mandible, ectotympanic, and stylohyal (all on the same scale) of *Arboroharamiya jenkinsi*. (B) The mandible, ectotympanic, and stylohyal (all on the same scale) of *Arboroharamiya allinhopson*. (C,D) Close-up view of the ectotympanic of *A. jenkinsi* (C) and *A. allinhopsoni* (D). (A–D) are not to scale. brk, breakage on the ectotympanic; cfm, contact area for the malleus; dt, dentary bone; etm, ectotympanic; rtm, ridge for attachment of the anterior part of the tympanic membrane; stl?, stylohyal?; ty-d, lateral ectotympanic part presumably equivalent to the dorsal part of the angular; ty-r, ectotympanic part presumably equivalent to the reflected lamina. Some images are flipped for convenience of comparison.

Auditory apparatus of euharamiyidans

Because of the similar stapes and incus in *A. jenkinsi* and *A. allinhopsoni* and the similar ectotympanic in *Arboroharamiya* and *Q. jizantang*, we postulate that the auditory apparatuses in these three species are similar. In these species, the auditory bones are fully detached from the dentary and are interpreted as having exclusively functioned for hearing. The detachment must have evolved independently of those in monotremes and therians given the current phylogeny of mammals (Luo et al. 2015; Han et al. 2017). Based primarily on the holotype of *A. allinhopsoni*, the auditory region (not including the inner ear) is reconstructed in comparison with those of other mammaliaform (Fig. 9). As described above, the stapes and incus are nearly in their anatomical position, and the malleus, ectotympanic, and surangular (MES) may have been slightly displaced. We interpret that the body of the malleus is most probably ventral to the incus and the anatomical orientation of the MES is inclined, parallel to the fenestra vestibuli, as inferred in other mammaliaforms (Wible, 1991; Allin & Hopson, 1992; Rougier et al. 1996); this orientation is consistent with that of the articular surface of the incudal body. The reconstructed orientation of the MES is intermediate between the nearly horizontal one in monotremes (Aitkin & Johnstone, 1972; Gates et al. 1974; Zeller, 1989, 1993) and the almost vertical one in *Didelphis* (Wible & Hopson, 1993; Figs 10 and 11). In the reconstruction (Figs 9 and 10), we have retained the preserved configuration of the MES, but it is highly probable that the bone relationship may have been slightly altered. We conclude that the MES would have functioned to support the tympanic membrane.
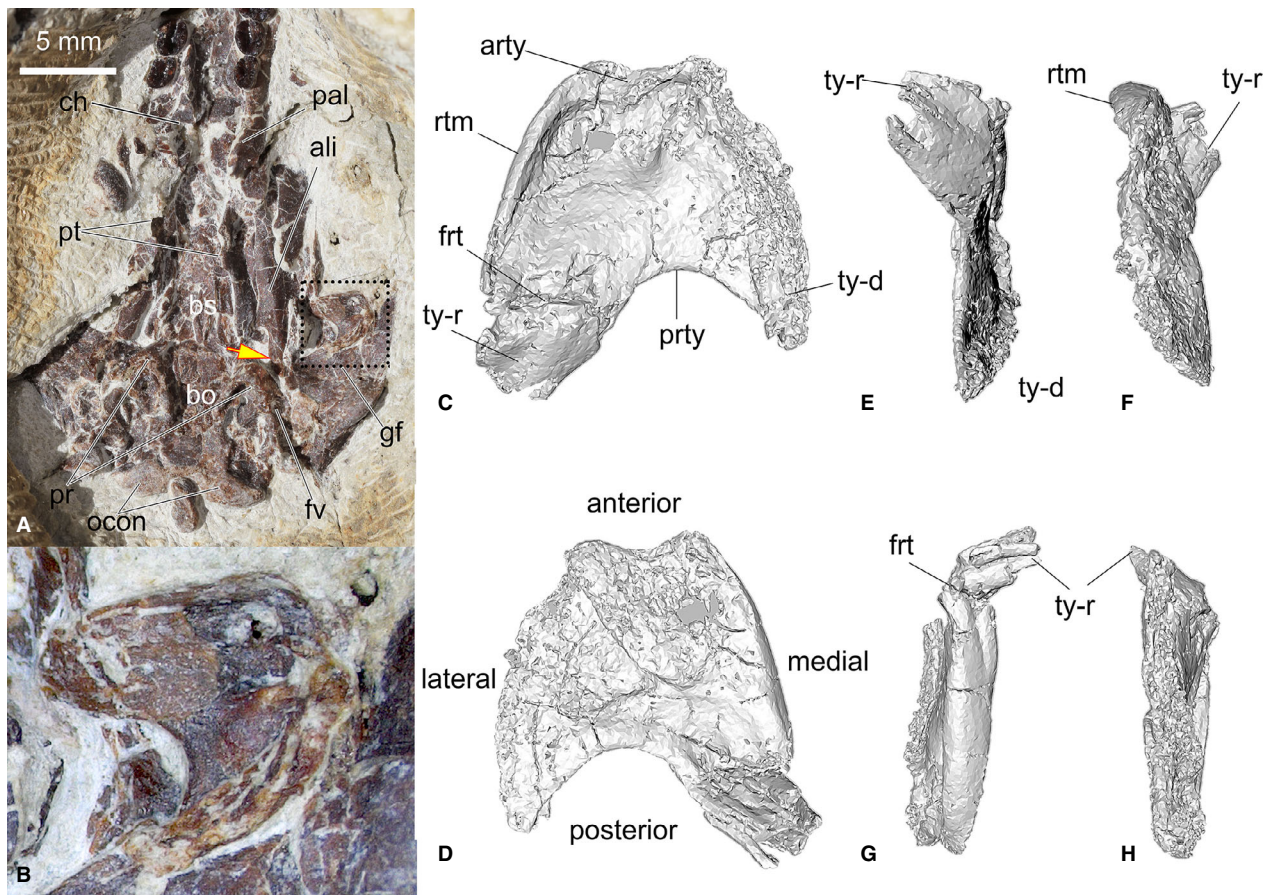
Fig. 8 The basicranial region and left ectotympanic of *Qishou jizantang* (holotype, JZT-D061). (A) Ventral view of the basicranial region. (B) Close-up of the ectotympanic bone, corresponding to the dash-lined boxed area in (A). The arrow points to the posterior end of the alisphenoid, similar to that of *Arboroharamiya allinhopsoni* (Fig. 1A,B). (C–H) Ventral, dorsal, posterior, anterior, medial, and lateral views of the ectotympanic. ali, alisphenoid; arty, anterior edge of the ectotympanic; bo, basioccipital; bs, basisphenoid; ch, choanae (internal nares); frt, fracture; fv, fenestra vestibuli; gf, glenoid fossa; ocon, occipital condyle; pal, palatine; pr, promontorium; prty, posterior edge of the ectotympanic; pt, pterygoid (hamulus); rtm, ridge for attachment of the anterior part of the tympanic membrane; ty-d, lateral ectotympanic part presumably equivalent to the dorsal part of the angular; ty-r, ectotympanic part presumably equivalent to the reflected lamina. (A,B) are modified from Mao & Meng (2019a).

Although the precise shape and size of the tympanic membrane is difficult to ascertain, it is clear that the area delimited by the MES is sufficiently large in relation to the area of the fenestra vestibuli. Coupled with the manubrium of the malleus, and the stapedial and lenticular processes of the incus, a leverage mechanism, as in mammals (Allin, 1975; Fleischer, 1978; Kermack et al. 1981; Manley & Sienknecht, 2013), had developed to transmit airborne sound vibrations from the tympanic membrane to the inner ear and amplify the sound pressure at the footplate of the stapes.

Because of the large PISM, it is probable that a sizable stapedius muscle was present. In extant mammals, tension of the stapedius muscle may function as protection of the inner ear from overstimulation or for change of the frequency response of the ear; in either case, the articulation between incus and stapes has to allow for some lateral give (Fleischer, 1978). Similar functions may be inferred for the stapes and the stapedius muscle of *Arboroharamiya*, but the large muscle suggests that the functions may not have been as sensitive as those of therians, particularly for high-frequency sounds.

The plate-like morphology is reminiscent of the plate-like angular bone in non-mammalian cynodonts (Fig. 10). The tympanic membrane would stretch along the anterior rim of the ectotympanic to the posterior rim of the malleus and surangular (Fig. 2) and the external auditory meatus would be located posterior to the glenoid fossa. In this regard, an alternative interpretation was provided by Dr. Edgar Allin (personal communication in an email to J.M., 26 November 2017): "The curved ridge on the anterior margin of the ectotympanic may have marked the end of the external auditory meatus rather than an attachment of the tympanic membrane. Given the flatness of the ectotympanic it may have been a vibratory ossicle rather than a static eardrum support. If so, it would have been part of the 'functional

tympanum' in addition to the tympanic membrane and manubrium". We agree that the ectotympanic may have functioned as a vibratory ossicle, similar to that in monotremes (Aitkin & Johnstone, 1972; Gates et al. 1974). The two interpretations, along with the interpretations of the manubrium, should be tested with additional evidence.
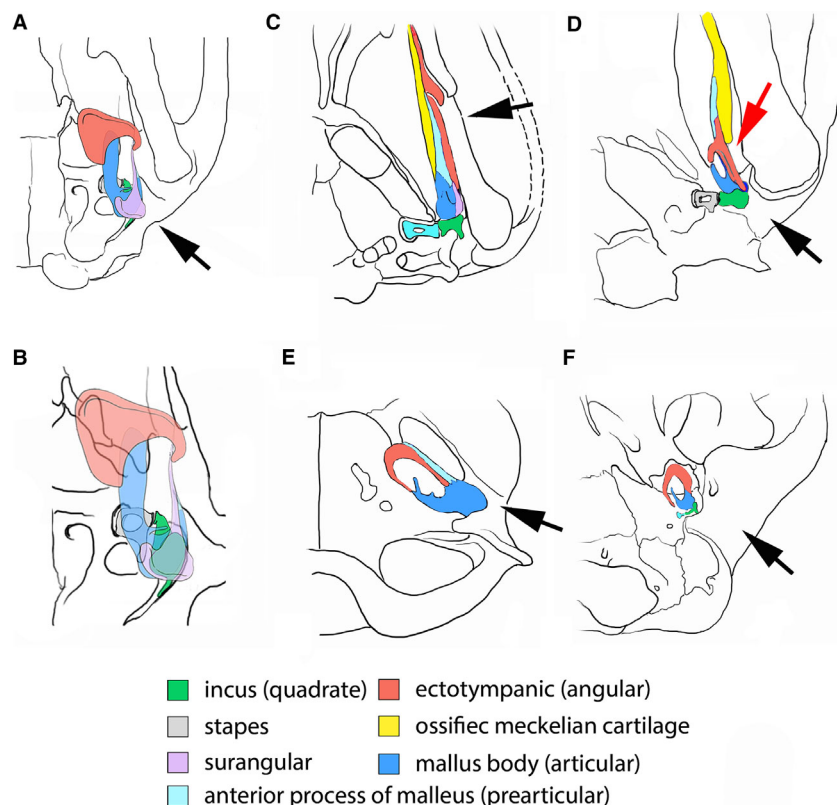
Compared with the bones in the MdME (Fig. 10), the detached auditory bones in *Arboroharamiya* are further reduced, reflecting the trend that leads to a refined auditory apparatus sensitive to high-frequency sounds (Allin, 1975, 1986; Bramble, 1978; Crompton & Parker, 1978; Kemp, 1982; Kermack & Kermack, 1984; Meng et al. 2003). On the other hand, because the auditory bones of *Arboroharamiya* are relatively massive in comparison with those of extant mammals (Doran, 1878; Segall, 1970; Henson, 1974; Fleischer, 1978), and the cochlea is curved but not coiled (Fig. 2), we infer that the hearing ability of *Arboroharamiya,* in terms of the sensitivity and range of frequency, may have been superior to that of *Morganucodon* (Kermack et al. 1981) and perhaps similar to that of monotremes (Aitkin & Johnstone, 1972; Gates et al. 1974) among extant mammals and possibly similar to that of multituberculates that have a similar cochlea (Luo & Ketten, 1991; Meng & Wyss, 1995; Fox & Meng, 1997; Hurum, 1998). It is unlikely that the hearing ability had reached to the level of the Mesozoic and extant therians in which the cochlea has coiled at least 360° (Meng & Fox, 1995a,b; Vater et al. 2004).

Comparison and Discussion

Arboroharamiya

The stapes of the two species of *Arboroharamiya* are characterized by having a rectangular outline with a large foramen and a robust PISM (Figs 3 and 4). However, differences do exist between them. The holotype of *A. jenkinsi* represents the largest known euharamiyidans, so that the absolute size of the stapes is considerably larger than that of *A. allinhopsoni*. The length of the stapes is 1.95 mm and the width at the midpoint of the stapes (without the process) is 1.06 mm in *A. jenkinsi,* which give a ratio of 1.84. The same ratio is 1.26 in *A. allinhopsoni* (1.2/0.95). This ratio indicates that the stapes of *A. jenkinsi* is transversely (from the footplate to the head) longer than that of *A. allinhopsoni*. Similarly, the stapedial foramen of *A. jenkinsi* is proportionally longer than that of *A. allinhopsoni*; in the former, the length (1.54 mm) to width (0.7 mm) ratio of the stapedial foramen is 2.2, whereas it is 1.51 in the latter (0.68/0.45). In *A. jenkinsi* the crura of the stapes are relatively slim and the PISM is plate-like with a broad base derived from the posterior crus and gradually tapers distally to end as a sharp tip. In contrast, the PISM in *A. allinhopsoni* is rod-like and ends bluntly (Fig. 4). Moreover, the stapedial head of *A. allinhopsoni* appears to be more distinctive and restricted (narrower) than that of *A. jenkinsi*.

Fig. 9 Comparison of the middle ear region of *Arboroharamiya* with other mammaliaforms. (A) The reconstructed middle ear of *Arboroharamiya* in ventral view. The auditory bones have been placed in an inclined position. (B) Close-up view of the auditory bones of *Arboroharamiya*, with the malleus, ectotympanic, and surangular displayed as semi-transparent so that other elements dorsal to them can be seen. (C–F) Ventral views of the basicranial and ear regions in *Morganucodon*, *Liaoconodon*, *Ornithorhynchus*, and *Didelphis*. The black arrow points to the external auditory meatus; the red arrow in (D) points to the gap between the ear ossicles and the dentary. (C–F) are modified from Meng et al. (2011) based on published works (Kermack et al. 1973; Allin, 1975; Allin & Hopson, 1992; Wible & Hopson, 1993; Zeller, 1993; Kielan-Jaworowska et al. 2004). The stapes in (D) has been modified based on Meng & Hou (2016). Some figures have been photographically flipped for convenience of comparison. Figures are not on the same scale, but the elements in each taxon are in proportion.
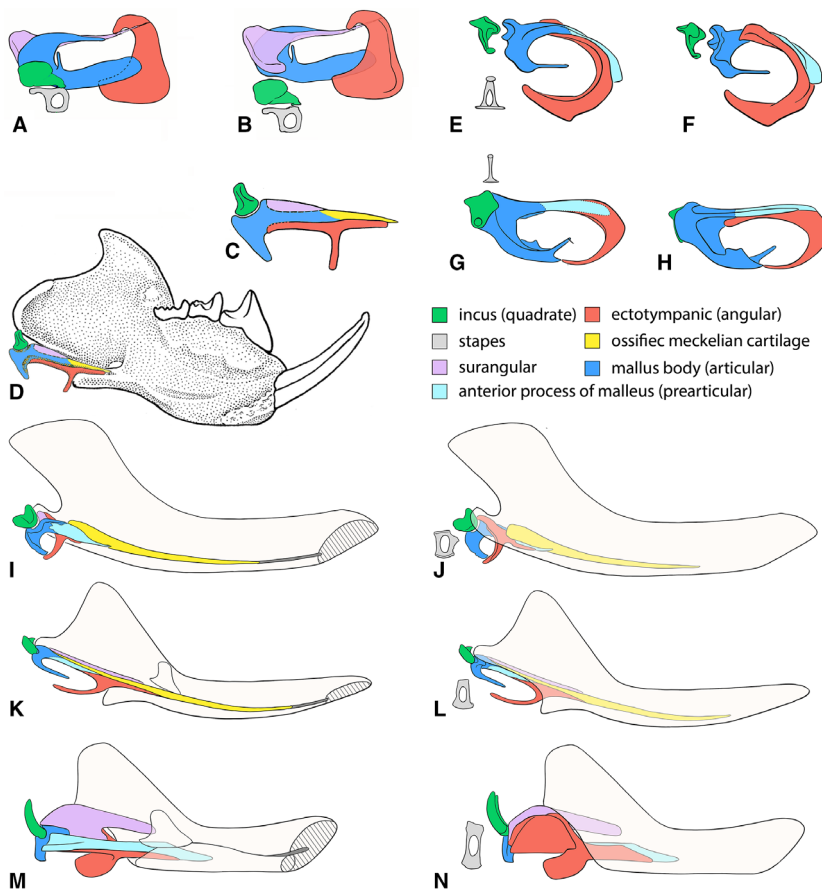

- incus (quadrate)
- stapes
- surangular
- anterior process of malleus (prearticular)
- ectotympanic (angular)
- ossifiec meckelian cartilage
- mallus body (articular)

Fig. 10 Comparison of the auditory bones of *Arboroharamiya* with other mammaliaforms. (A,B) Dorsal (medial) and ventral (lateral) views of the auditory bones. The positions of the bones in (A) are our interpretation. (C,D) Auditory bones (postdentary elements) and their attached position at the dentary in *Vilevolodon*. (E,F) Dorsal (medial) and ventral (lateral) views of the auditory bones (the stapes is in lateral view) of *Didelphis*. (G,H) Dorsal (medial) and ventral (lateral) views of the auditory bones (the stapes is in lateral view) of *Ornithorhynchus*. (I–N) Medial-lateral views of the auditory (postdentary) bones (the stapes is in lateral view) of *Liaoconodon*, *Morganucodon*, and *Thrinaxodon*. All figures are modified from Han et al. (2017), except for (C) and (D), based on published work (Allin, 1975; Zeller, 1993; Meng et al. 2011). The stapes in (J) is based on Meng & Hou (2016). (C) and (D) are modified from Luo et al. (2017). Some figures have been flipped for convenience of comparison. Figures are not on the same scale.

Legend:
- incus (quadrate)
- stapes
- surangular
- anterior process of malleus (prearticular)
- ectotympanic (angular)
- ossifiec meckelian cartilage
- mallus body (articular)

Although the stapedial process of the incus in *A. jenkinsi* does not seem preserved, the bulbous body with a rounded articular surface for the malleus, the slim short process, and the 'network' within the bone are nearly identical in the incus of the two species, and these configurations appear to be unique. The incus is similar to that of therians in possessing stapedial and lenticular processes, which differ from those of monotremes and other mammaliaforms (Fig. 10).

Compared with the stapes and incus, the malleus of *A. allinhopsoni* is more incompatible with those known in other mammaliaforms (Figs 9 and 10). The anterior process of the malleus in *A. allinhopsoni* is short and the medial process robust; the latter is unique to *A. allinhopsoni*, and is unknown in any mammals. The manubrium of the malleus in *A. allinhopsoni* is a slim bony prong, similar to that of extant mammals but different from that interpreted for *Vilevolodon* (Luo et al. 2017; see below). Because the robust medial process in *A. allinhopsoni* was interpreted as homologous to the retroarticular process of the articular, the manubrium in *A. allinhopsoni* was interpreted as evidence supporting it as a neomorphic structure (Allin & Hopson, 1992; Clack & Allin, 2004; Meng et al. 2011), which was also echoed by developmental studies (Fleischer, 1973; Presley, 1984; Mallo, 2001; Sánchez-Villagra et al. 2002; Takechi & Kuratani, 2010). However, the alternative interpretation by

Dr. Allin suggests a large manubrium (see above), which, if true, is also unique among mammaliaforms.

The ectotympanic in the two species of *Arboroharamiya* is plate-like and the portion homologous to the reflected lamina of the angular is broad. In addition, it has a short posterior limb but lacks an anterior limb. There are some minor differences in the ectotympanic of the two species.

The general morphology of the surangular in *A. jenkinsi* is similar to that of *A. allinhopsoni*, with a fan-shaped body and a needle-like process (Fig 6c,g). As we reported above, the surangular is preserved on the ventral side of the malleus in *A. allinhopson* and, if positioned vertically, it would be lateral to the malleus, consistent in position with the surangular of *Morganucodon* that supplied the major part of the firm attachment between the dentary and the articular complex (Kermack et al. 1973). Reduction of the surangular was considered a major step toward separation of the postdentary elements from the dentary, which freed more area on the medial surface of the dentary for attachment of jaw muscles (see Meng et al. 2011 for a brief review). This posterior surface of the body is reminiscent of an articular surface and is here interpreted as being the remnant surangular boss; the latter articulated with the initial glenoid fossa of the squamosal in some non-mammalian cynodonts (Crompton, 1972; Allin, 1975; Crompton & Jenkins, 1979).

Fig. 11 Reconstructed CT images showing the relationship of the mandible, middle ear, and the cranium in *Qishou* (JZT-D061). (A) Lateral view of the mandible and the cranium part. (B) Medial view of the mandible (with the lateral view of the cranium). (C–D) Posterodorsal view of the posterior half of the mandible, showing the mandibular foramen, the groove extending from it, and the possible location of the 'ectotympanic' as interpreted by Luo et al. (2017). agp, angular process; cop, coronoid process; gf, glenoid fossa; gmf, groove leading from the mandibular foramen; mc, mandibular condyle; mdf, mandibular foramen; ptf, pterygoid fossa; pm, promontorium; vrpf, ventral ridge of the pterygoid fossa; za, zygomatic arch.
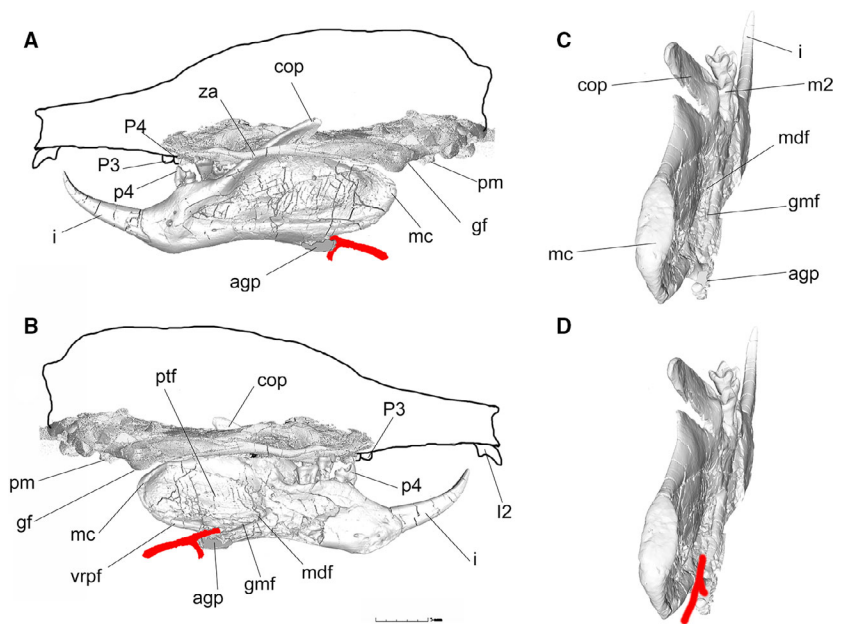
Qishou

Only the ectotympanic is preserved in the holotype of *Q. jizantang* (Mao & Meng, 2019a; Fig. 8). Its similarities to and differences from those of *Arboroharamiya* have been reported above. The importance of this specimen is that, in association with the basicranial structures, the completeness, shape, and size of the ectotympanic show that it cannot be any other bone or part of another bone in the skull, such as the pterygoid hamulus. The similar morphology of the ectotympanic in *A. jenkinsi, A. allinhopsoni*, and *Qishou* suggests a similar middle ear in the three species.

Vilevolodon

Vilevolodon was dentally similar to other euharamiyidans from the Yanliao Biota (Zheng et al. 2013; Bi et al. 2014; Mao & Meng, 2019a; Mao et al. 2019), but its reconstructed auditory apparatus is distinctive from that of *Arboroharamiya* (Luo et al. 2017; Fig. 10).

The stapes is not preserved in *Vilevolodon*. As reported by Luo et al. (2017, supplementary information): 'The right incus is compressed onto the right malleus, while the left incus, as rendered from CT scans, shows a trochlea and a dorsal process similar to those of *Sinoconodon* and *Morganucodon*. We tentatively interpret that the incus lacks an independent stapedial process'. In addition to the considerable morphological difference, the incus of *Vilevolodon* was positioned posterodorsally to the body of the malleus (Fig. 11). The relationship of the incus with the stapes is unknown, but presumably the medial side of the distal portion (the dorsal process) of the incus would articulate with the stapes.

The malleus of *Vilevolodon* has an anterior process that was interpreted as a shortened ossified Meckel's cartilage or a prearticular. The malleus body has a concave articular facet for the incus. In addition, the malleus of *Vilevolodon* bears a broad process that was interpreted as the manubrium and a large sliver of bone, attached to the posterior end of Meckel's cartilage, was tentatively interpreted to be a surangular. Thus, the malleus, the ossified Meckel's cartilage, and the prearticular are preserved in one unit in *Vilevolodon* (Luo et al. 2017; Fig. 10). The putative surangular is on the dorsal side of the malleus and does not nestle, or very little if at all, in the postdentary trough (Luo et al. 2017: fig. 3g; extended data fig. 9b). The general morphology of the left malleus is similar to the element identified as the surangular in *A. allinhopsoni*. It is interesting to note that the right malleus body and 'compressed surangular+prearticular' appears to be one element (Luo et al. 2017: figs S3, S8a, b), with its lateral portion broken, and the element appears different from the left malleus. Instead, the malleus body is similar to that of *A. allinhopsoni* and the 'surangular+prearticular' as a whole is similar to the medial process of the malleus in *A. allinhopsoni*.

The ectotympanic of *Vilevolodon* has an anterior limb, a posterior limb, and a gracile and straight portion (=reflected lamina of the angular) (Luo et al. 2017). The anterior limb and the short Meckel's element (or prearticular) were interpreted as being nestled in a short and triangular postdentary trough between the inflected angular process and the vertical plate of the mandible (Luo et al. 2017). A similar bone in *Arboroharamiya* is identified as the stylohyal (see above). Regardless of their identification, these two bones are similar in several aspects: they are slim, with the anterior process being shorter than the posterior one; the posterior process flares posteriorly; the lateral process (the straight portion of Luo et al. 2017) forms an angle < 90° to the anterior process and its tip shows a tendency to bend posteriorly.

In short, except for the unknown stapes, the auditory apparatus of *Vilevolodon* is drastically different from that of *Arboroharamiya* (Fig. 10). The complex is presumably still attached to the dentary and none of the elements in the complex are comparable to the corresponding ones in *Arboroharamiya*. As interpreted, the middle ear of *Vilevolodon* is more similar to that of *Morganucodon* than to the transitional mammalian middle ear as represented by *Liaoconodon* (Meng et al. 2011; Fig. 10) and the definitive mammalian middle ear of extant mammals (Figs 9 and 10).

Multituberculates

Multituberculates are possibly related to 'haramiyidans' as allotherians (Kielan-Jaworowska et al. 2004), although phylogenetic hypotheses for these groups remain diverse. While most recent phylogenetic analyses clustered 'haramiyidans' with multituberculates, probably including gondwanatherians as well, and placed this group in Mammalia (Luo et al. 2002; Luo & Wible, 2005; Luo et al. 2007a, b; Rowe et al. 2008; Ji et al. 2009; Luo et al. 2011; Meng et al. 2011; Zheng et al. 2013; Bi et al. 2014; Krause et al. 2014; Meng et al. 2018; Han et al. 2017), other studies alternatively placed the group outside of mammals (Luo et al. 2015, 2017; Huttenlocker et al. 2018). The evidence that supports the allotherians as consisting of multituberculates and 'haramiyidans' mainly comes from the dentition, such as the presence of only two upper and lower molars (except for *Haramiyavia*), two rows of multiple cusps on the molars, and a single and enlarged lower incisor. The elongate and curved cochlea in *A. allinhopsoni* (Han et al. 2017) is also similar to that of multituberculates (Luo & Ketten, 1991; Meng & Wyss, 1995; Fox & Meng, 1997; Hurum, 1998), but a similar condition also exists in other groups (Ruf et al. 2009; Panciroli et al. 2019).

Auditory bones of multituberculates were poorly known from fragmentary material (Miao & Lillegraven, 1986; Meng, 1992; Meng & Wyss, 1995; Hurum et al. 1996; Rougier et al. 1996; Schultz et al. 2018) such that convincing evidence has yet to be established supporting the middle ear of multituberculates. Nonetheless, those fragmentary specimens do show differences from the auditory bones of *A. allinhopsoni*. For instance, the ectotympanic of *Lambdopsalis* has a tympanic sulcus for holding the tympanic membrane (Meng & Wyss, 1995). The partial stapes of *Pseudobolodon* represents the only and earliest known middle ear bone of Late Jurassic multituberculates (Schultz et al. 2018). The reconstruction of the asymmetric bicrural stapes is more similar to that of a therian but differs from *Arboroharamiya*. This reconstruction implies that the stapes was probably flexible so that the posterior crus could bend and the foramen widen. This elasticity may be unfavorable for transmitting sound vibrations. The reconstructed stapes is shorter than the maximum diameter of the footplate, an uncommon condition in mammaliaforms. The reconstructed stapes also lacks the PISM, implying that the stapedius muscle was either absent or so small that it would have inserted on the stapedial head. In multituberculates, such as *Kryptobaatar*, the fossa for the stapedius muscle is broad, at least twice the surface area of the fenestra vestibuli (Wible & Rougier, 2000), which implies that the stapedius muscle in multituberculates was present and probably sizable. With all these concerns, an alternative and simpler interpretation we offer here is that the preserved stapes of *Pseudobolodon* more or less retained the original morphology in which the purported stapedial head can be interpreted as the PISM, similar to that of *Chaoyangoden* (Meng & Hou, 2016), but the anterior crus and the actual stapedial head were broken. However, the alternative interpretation, if true, does not necessarily provide evidence for the affinity of multituberculates and 'haramiyidans', because a stapes with a distinct PISM is also present at least in eutriconodontans and may represent a primitive feature of mammals.

Monotremes (*Ornithorhynchus*)

The middle ear of monotremes is morphologically different from those of therians (Doran, 1878; Aitkin & Johnstone, 1972; Fleischer, 1973; Gates et al. 1974; Zeller, 1989, 1993) and *Arboroharamiya* (this study) in several aspects. The stapes of monotremes is T-shaped (monocrurate) and lacks a PISM (Fig. 11). As postulated by Meng & Hou (2016), this lack is because monotremes do not have the stapedial muscle (Fleischer, 1978). Instead, the levator hyoidei muscle, from which the stapedius muscle is derived, is present in monotremes (Edgeworth, 1931, 1935; Wible, 1991; Wible & Hopson, 1993).

The incus is a flat little plate (Fig. 11) that tightly abuts or is even ankylosed to the dorsal side of the transverse part of the malleus (Aitkin & Johnstone, 1972; Gates et al. 1974; Zeller, 1993), as reported by Doran (1878: p. 488 for *Echidna hystrix*): 'Hence the incus is articulated to the malleus by its whole inner surface, including the greater part of its long crus, and also by its convex inferior border. It is firmly ankylosed to the malleus; and even in a young skull the ossicles cannot be separated uninjured without difficulty'.

The malleus has a long anterior process and a manubrium that points anteriorly (Doran, 1878; Zeller, 1993; Fig. 10). The ectotympanic is sickle-shaped and bears a tympanic sulcus for holding the tympanic membrane; it is also tightly connected to the long anterior process of the malleus by soft tissue (Aitkin & Johnstone, 1972; Gates et al. 1974; Zeller, 1993). In general, the middle ear morphology of monotremes is different from those of *Arboroharamiya* and therians, except that the auditory bones are detached from the dentary.

Therians (*Didephis*)

In therian mammals, auditory bones display a variety of morphologies (Doran, 1878; Segall, 1970; Henson, 1974;

Fleischer, 1978; Novacek & Wyss, 1986; Novacek, 1993), and those of *Didephis* may represent a general pattern of therians. All the auditory bones of *Arboroharamiya* are proportionally more robust than those of *Didephis* (Fig. 10). In contrast to other mammaliaforms (Fig. 11), a common feature of the stapes is that the stapedial head is distinctively narrower than the footplate and articulates with the similarly restricted lenticular process of the incus, a configuration considered to be a derived condition for mammals (Meng, 1992; Meng & Hou, 2016). The PISM is either extremely small, interpreted as representing a vestige of the ossified proximal base of the interhyal (Meng & Hou, 2016), or indiscernible, so that the stapedius muscle inserts directly on the head of the stapes (Doran, 1878; Segall, 1970; Henson, 1974; Fleischer, 1978; Novacek & Wyss, 1986). In anatomical position, the incus is generally posterior to the malleus (Doran, 1878; Segall, 1970; Fleischer, 1973; Henson, 1974; Sánchez-Villagra et al. 2002). Although the incus of *Arboroharamiya* develops the stapedial and lenticular processes, these processes in therians are relatively slim and long. In addition, the articulation for the malleus is saddle-shaped, not a simple convex facet. The ectotympanic is commonly horseshoe-shaped, bears a tympanic sulcus, and is intimately attached (or even synostosed) to the long anterior process of the malleus (Fig. 10).

Eutriconodontans (*Liaoconodon*)

Within eutriconodontans, the holotype of *Liaoconodon* preserves unequivocal middle ear bones (except for the stapes) in articulation with Meckel's cartilage, illustrating the transitional mammalian middle ear (TMME, Meng et al. 2011) or partial mammalian middle ear (Luo, 2011) in which the auditory bones have detached from the dentary but still are connected by Meckel's cartilage (Fig. 10). The TMME appears to be common in eutriconodontans (Wang et al. 2001; Meng et al. 2003, 2011; Luo et al. 2007a) and 'symmetrodontans' (Meng et al. 2003; Ji et al. 2009), as evidenced by the presence of the ossified Meckel's cartilage (OMC) or of the Meckelian groove on the medial rear surface of the dentary (Meng et al. 2003).

An unequivocal eutriconodontan stapes is known from *Chaoyangoden* (Hou & Meng, 2014; Meng & Hou, 2016; Fig. 10). The PISM on the stapes of *Chaoyangoden* is considerably smaller than that in *Arboroharamiya* but is still conspicuous, larger than that in extant therians. The incus of *Liaoconodon* has neither a long stapedial process nor a lenticular process (Fig. 11); lack of the lenticular process is consistent with the unrestricted head of the stapes of *Chaoyangoden*. The malleus of *Liaoconodon* has a long anterior process (including the prearticular) that partly wraps around the ossified Meckel's cartilage. The articulation between the malleus and incus is hinge-like, with the incus positioned posterior to the malleus. The malleus lacks a manubrium and its ventrally projected manubrial base

was homologized to the retroarticular process in basal mammaliaforms (Meng et al. 2011). The ectotympanic is three-pronged, with a short ventral process (equivalent to the reflected lamina) in comparison with that of extant mammals. Still, the ectotympanic is more similar to those of extant mammals than to that of *Arboroharamiya* (Fig. 11). A process on the malleus of *Liaoconodon* was interpreted by Meng et al. (2011) as the surangular boss (Crompton, 1972; Allin, 1975), but its homology to the surangular remains uncertain. In general, the TMME as represented by *Liaoconodon* is notably different from the middle ear of *Arboroharamiya*.

Basal mammaliaforms (*Morganucodon*)

The auditory region of *Morganucodon* represents the typical mandibular middle ear (MdME) in basal mammaliaforms and has been widely referred to in studies on the evolution of the mammalian middle ear (Kermack et al. 1973, 1981; Allin, 1975; Allin & Hopson, 1992). A similar configuration has at least been known in docodontans (Lillegraven & Krusat, 1991; Ruf et al. 2013). *Hadrocodium* (Luo et al. 2001) was considered to have the DMME, an example supporting brain expansion as the mechanism for detachment of the postdentary bones in mammalian evolution (Rowe, 1996). This opinion on *Hadrocodium* has been questioned (Wang et al. 2001; Meng et al. 2003) and in a recent study (Luo et al. 2016), *Hadrocodium* was reinterpreted as having a shallow postdentary trough and Meckel's sulcus, thus a MdME. Compared with those in non-mammaliaform cynodonts, the postdentary bones in the MdME are reduced in size but still attached to the dentary. The primary articulation between the articular (malleus) and quadrate (incus) co-exists with the secondary squamosal-dentary joint (Fig. 10) so that the postdentary bones had dual function for both mastication and hearing. However, due to the poor fossil record, detailed morphologies of the stapes, articular and prearticular (malleus), and angular (ectotympanic, particularly the reflected lamina) are still equivocal. For instance, whether the stapes has a PISM, whether the malleus possesses a manubrium, and what the exact shape of the reflected lamina is, need to be demonstrated with better fossil evidence.

Non-mammaliaform cynodonts (*Thrinaxodon*)

In non-mammaliaform cynodonts, such as *Thrinaxodon* (Fig. 11), there is only the primary jaw joint between the articular in the lower jaw and the quadrate in the cranium. All the postdentary bones are proportionally large. Although the general homology of the mammalian middle ear bones with their precursors was established long ago (Reichert, 1837; Gaupp, 1913) and has been extensively studied (Doran, 1878; Van Kampen, 1905; Palmer, 1913; Goodrich, 1930; Olson, 1944; Allin, 1975; Maier, 1990; Zeller,

1989, 1993), evolutionary and developmental issues on detailed structures of the auditory bones still exist. An example is the relationship of the dorsal process on the stapes in some non-mammaliaform therapsids (Watson, 1953; Hopson, 1966; Allin, 1975; Parrington, 1979; Allin & Hopson, 1992; Rodrigues et al. 2013; Ruf et al. 2013; Gaetano & Abdala, 2015) and the PISM in mammals (Doran, 1878; Fleischer, 1973; Novacek & Wyss, 1986). The dorsal process, was interpreted as the attachment site for the stapedial muscle (Gaetano & Abdala, 2015), although not in *Thrinaxodon* (Fig. 11), which raises the homology issue of the dorsal process and the PISM that remains to be addressed (Meng & Hou, 2016; Meng et al. 2018).

Ectotympanic vs. stylohyal

Puzzling issues have been arisen from recent discoveries of euharamiyidan skeletal material from the Jurassic Yanliao Biota, China (Zheng et al. 2013; Zhou et al. 2013; Bi et al. 2014; Meng et al. 2014, 2017; Han et al. 2017; Luo et al. 2017). These include the dental occlusal patterns (Meng et al. 2014, 2017; Luo et al. 2015) and the configuration of the auditory bones (Han et al. 2017; Luo et al. 2017); both affect outcomes of higher-level phylogenetic analyses involving 'haramiyidans'. The occlusal patterns of 'haramiyidans' have been discussed elsewhere (Mao & Meng, 2019a, b), and here we present further discussion about the auditory bones. The key issue centers on the different auditory apparatus represented by *Vilevolodon* and *Arboroharamiya*; the former is reported as having a mandibular middle ear, whereas the latter possesses a definitive mammalian middle ear (Fig. 11). *Vilevolodon* and *Arboroharamiya* are dentally similar and taxonomically closely related; they co-existed in the same locality of the Jurassic Yanliao Biota. The pivotal question is why they differ so much in their auditory apparatus. One possible answer is that the auditory bones may be re-interpreted differently. Of the elements identified as ear bones, only one is morphologically comparable: the element identified as the ectotympanic in *Vilevolodon* (Luo et al. 2017; Fig. 10); however, here we regard it as the stylohyal. For convenience in the discussion on the two interpretations, we call this element the X-bone.

CL images of the X-bones in *Arboroharamiya* and the CT-rendered X-bone in *Vilevolodon* show thin elements, each bearing a lateral process (or the reflected lamina of Luo et al. 2017). In *Arboroharamiya* the lateral process leans anteriorly with its tip bending posteriorly. The lateral process in *Vilevolodon* has a similar anterior tilt (Luo et al. 2017: extended data fig. 8a,b), but in the reconstruction of the auditory apparatus, it seems to lean slightly posteriorly. The posterior process in the X-bone of *Vilevolodon* also shows a tendency to flare posteriorly, similar to that in *Arboroharamiya* (Figs 5 and 7).

The preserved locations of the X-bone in *Vilevolodon* and *A. allinhopsoni* are similar, both being near the angular process of the dentary. Luo et al. (2017): extended data figs 2, 3, and 8) considered the X-bone in *Vilevolodon* to have been preserved *in situ*; it is closely associated with other auditory elements as well as the basihyal and epihyal. A similar element is present by the angular process in *Xianshou linglong* and was identified as a hyoid element (Bi et al. 2014: extended data figure 5b). The X-bone in *A. jenkinsi* is associated with a possible epihyal (Figs 5D and 6), although both are floating elements in the preserved state.

It is intriguing that the X-bone co-exists with the five elements identified as auditory bones, including the ectotympanic, in the holotype of *A. allinhopsonii,* and with the ectotympanic in the holotype of *A. jenkinsi.* Assuming the homology of the X-bone in *Vilevolodon* and *Arboroharamiya*, regardless of detailed differences, identification of the X-bone as the ectotympanic in *Vilevolodon* ought to be questioned. Here we would suggest that the X-bone is probably not the ectotympanic but a hyoid element, most likely the stylohyal.

In relation to the massive lower jaw (Fig. 10), the X-bone is too slim and small to be an ectotympanic (angular) still attached to the dentary. The anterior process is too short and weak to be the supporting structure that attaches the auditory apparatus to the dentary. Its lateral and posterior processes show no tympanic sulcus or any structure that indicates the attachment of the tympanic membrane. The lateral process inclines anteriorly, forming an angle of 80° with the anterior process. If the X-bone was the ectotympanic, the lateral process would be homologous to the reflected lamina of the angular. In other mammaliaforms, the reflected lamina or its equivalent inclines posteriorly and forms a larger angle (> 90°) with the anterior limb of the ectotympanic (Fig. 10); the orientation of the reflected lamina is opposite to that of *Arboroharamiya* and *Vilevolodon*. The anterior inclination of the lateral process hampers the attachment of the X-bone to the dentary. If the X-bone was the ectotympanic, the area delimited by the posterior process and the lateral process is too small to hold a functional tympanic membrane.

As preserved, the stapes and incus are nearly in their anatomical position in the holotype of *A. allinhopsoni*, and the upper and lower teeth are in occlusion. If the X-bone was nestled in the postdentary trough, there is a distance between it and the middle ear region (Figs 9 and 11); it is impossible that the X-bone could have been in contact with the auditory bones that are associated with the promontorium and the fenestra vestibuli while the upper and lower teeth are engaged. In addition, the groove that extends from the mandibular foramen to the notch between the angular process and the body of the mandible is narrow and even in its width, and does not have the shape of a postdentary trough (Mao & Meng, 2019a; Fig. 11).

Moreover, different from basal mammaliaforms, such as morganucodontids and docodonts, the mandible of euharamiyidans is deep, with the condyle being vertically extended so that the space between the groove and the ear region (e.g. the promontorium) is so large that a mandibular middle ear would not reach the incus that is lateral to the fenestra vestibuli (Figs 9 and 11). The groove directs posteroventrally; thus, if the X-bone was nestled in that groove, it would extend posteroventrally away from the mandibular condyle and be further separated from the middle ear region (Fig. 11). A similar condition is at least present in *Xianshou* (Bi et al. 2014: extended data figures 5c, 6b) and *A. jenkinsi* (Meng et al. 2014: fig. 2) where the medial side of the lower jaw is visible.

How the reconstructed mandibular middle ear in 'haramiyidans' worked remains a challenging issue (Meng et al. 2014). Except for *Theroteinus* (Sigogneau-Russell et al. 1986; Debuysschere, 2016), all 'haramiyidans' were interpreted as having a palinal phase during the chewing cycle. As the lower jaw moved posteriorly in chewing, the mandibular middle ear must have moved posteriorly along with the dentary; this would create a mechanical problem for the connection of the auditory bones in relation to the fenestra vestibuli. As shown in the holotype of *A. allinhopsoni*, it is clear that the incus body is lodged in the basicranial region and its lenticular process has a narrow articulation with the stapes; these features show that the incus could not move or rotate except when transmitting sound vibrations. Given the reconstruction in which the incus is attached to the posterodorsal end of the malleus in *Vilevolodon* (Fig. 10C,D), it appears also difficult for the malleus to move posteriorly while the incus remained in articulation with the stapes.

As an alternative interpretation, the X-bone may actually be a hyoid element, probably the stylohyal. Although hyoids are generally poorly studied in mammals (Shoshani et al. 2007), for those that are known, the hyoid bones show diverse morphologies among different groups of mammals (Inuzuka et al. 1975; Weissengruber et al. 2002; Takada et al. 2009; Simmons et al. 2010; Veselka et al. 2010; Wible, 2010; Casali & Perini, 2017). The hyoid apparatus functions as a suspensory mechanism for the tongue and larynx; thus, this apparatus attaches ventrally to the larynx and the base of the tongue, and suspends these structures in the caudal part of the space between the bodies of the mandibles (Evans & De Lahunta, 2013). The hyoid elements are commonly positioned near the angular process of the mandible in extant mammals (Inuzuka et al. 1975; Weissengruber et al. 2002; Takada et al. 2009; Pérez et al. 2010; Andrei et al. 2013) and in Mesozoic mammals (Bi et al. 2018). Similar to the mammalian condition and as preserved perhaps *in situ* in *A. allinhopsoni* and *Vilevolodon*, the stylohyal is more closely associated with the angular process of the dentary than to the middle ear region.

Conclusion

The auditory apparatus of euharamiyidans is best known in *Arboroharamiya*, which is preserved nearly in anatomical position. Among the five bones, the stapes and incus are most unambiguous because of their morphologies and nearly *in situ* preservation. Still, even these two bones are highly different from those of other known mammaliaforms. The malleus and ectotympanic are even more unusual compared with the corresponding elements in known mammaliaforms, not to mention the unique surangular. These peculiar morphologies are further complicated by the co-existing hyoid elements in the same individual and by different interpretations of the same element in *Vilevolodon*, such as the stylohyal in this study. Although we present the arguments for the interpretation we prefer, it is inevitable that these interpretations are subject to future rigorous tests with additional evidence. The current evidence already shows that 'haramiyidans' still remain a poorly known Mesozoic group and their auditory apparatuses are unique among mammaliaforms, which further shows that the evolution of the mammalian middle ear is much more complicated than previously known.

Acknowledgements

Conflicts of interest

The authors do not have any conflicts of interest to declare.

Authors' contributions

J.M. and F.M. designed the study. J.M. drafted the manuscript. F.M. performed CT and CL imaging and made the figures. G.H., X.Z., L.W., and Y.W. provided curation of the studied specimens and assisted with acquisition of related data. All authors contributed to the manuscript by comments in discussions during the course of the study.

References

Aitkin LM, Johnstone BM (1972) Middle-ear function in a monotreme: the echidna (*Tachyglossus aculeatus*). *J Exp Zool* **180**, 245–250.

Allin EF (1975) Evolution of the mammalian middle ear. *J Morphol* **147**, 403–437.

Allin EF (1986) The auditory apparatus of advanced mammal-like reptiles and early mammals. In: *The Ecology and Biology of Mammal-like Reptiles* (eds Hotton N, MacLean PD, Roth JJ, Roth EC), pp. 283–294. Washington, DC: Smithsonian Institution Press.

Allin EF, Hopson JA (1992) Evolution of the auditory system in Synapsida ('mammal-like reptiles' and primitive mammals) as seen in the fossil record. In: *The Evolutionary Biology of Hearing* (eds Webster DB, Popper AN, Fay RR), pp. 587–614. New York: Springer.

Andrei F, Motoc A, Didilescu A, et al. (2013) A 3D cone beam computed tomography study of the styloid process of the temporal bone. *Folia Morphol* **72**, 29–35.

Bi S-D, Wang Y-Q, Guan J, et al. (2014) Three new Jurassic euharamiyidan species reinforce early divergence of mammals. *Nature* **514**, 579–584.

Bi S-D, Zheng X-T, Wang X-L, et al. (2018) An early cretaceous eutherian and the placental–marsupial dichotomy. *Nature* **558**, 390–395.

Bramble DM (1978) The origin of the mammalian feeding complex: models and mechanisms. *Palaeobiology* **4**, 271–301.

Casali DM, Perini FA (2017) The evolution of hyoid apparatus in Xenarthra (Mammalia: Eutheria). *Hist Biol* **29**, 777–788.

Clack JA, Allin EF (2004) The evolution of single- and multiple-ossicle ears in fishes and tetrapods. In *Evolution of the Vertebrate Auditory System. Springer Handbook of Auditory Research, vol 22*. (eds Manley GA, Fay RR, Popper AN), pp. 128–163. New York: Springer.

Crompton AW (1972) The evolution of the jaw articulation of cynodonts. In: *Studies in Vertebrate Evolution* (eds Joysey KA, Kemp TS), pp. 231–251. Edinburgh: Oliver & Boyd.

Crompton AW, Jenkins FA Jr (1979) Origin of mammals. In: *Mesozoic Mammals: The First Two-thirds of Mammalian History* (eds Lillegraven JA, Kielan-Jaworowska Z, Clemens WA Jr), pp. 59–73. Berkeley: University of California Press.

Crompton AW, Parker P (1978) Evolution of the mammalian masticatory apparatus. *Am Sci* **66**, 192–201.

Debuysschere M (2016) A reappraisal of *Theroteinus* (Haramiyida, Mammaliaformes) from the Upper Triassic of Saint-Nicolas-de-Port (France). *PeerJ* **4**, e2592.

Doran AHG (1878) Morphology of the Mammalian Ossicula auditûs.. *Trans Linn Soc Lond*. *2nd Series: Zoology* **1**, 371–497.

Edgeworth FH (1931) On the development of the external ocular, masticatory, and hyoid muscles of Monotremata. *Proc Zool Soc London* **101**, 809–815.

Edgeworth FH (1935) *The Cranial Muscles of Vertebrates*. Cambridge: Cambridge University Press.

Evans HE, De Lahunta A (2013) *Miller's Anatomy of the Dog, E-Book*. Elsevier Health Sciences.

Fleischer G (1973) Studien am Skelett des Gehörorgans der Säugetiere, einschließlich des Menschen. *Säugetierkundliche Mitteilungen* **21**, 131–239.

Fleischer G (1978) *Evolutionary Principles of the Mammalian Middle Ear*. Berlin: Springer-Verlag.

Fox RC, Meng J (1997) An X-radiographic and SEM study of the osseous inner ear of multituberculates and monotremes (Mammalia): implications for mammalian phylogeny and evolution of hearing. *Zool J Linn Soc* **121**, 249–291.

Furutera T, Takechi M, Kitazawa T, et al. (2017) Differing contributions of the first and second pharyngeal arches to tympanic membrane formation in the mouse and chick. *Development* **144**, 3315–3324.

Gaetano LC, Abdala F (2015) The stapes of gomphodont cynodonts: insights into the middle ear structure of non-mammaliaform cynodonts. *PLoS ONE* **10**, e0131174.

Gates GR, Saunders JC, Bock GR, et al. (1974) Peripheral auditory function in the platypus, *Ornithorhynchus anatinus*. *J Acoust Soc Am* **56**, 152–156.

Gaupp EWT (1913) *Die Reichertsche theorie: (Hammer-, amboss- und kieferfrage)*. Arch Anat Entwicklungsgeschichte, Veit & Comp.

Goodrich ES (1930) *Studies on the Structure and Development of Vertebrates*. London: Macmillan and Co.

Han G, Mao F-Y, Bi S-D, et al. (2017) A Jurassic gliding euharamiyidan mammal with an ear of five auditory bones. *Nature* **551**, 451–456.

Henson OW Jr (1974) Comparative anatomy of the middle ear. In: *The Handbook of Sensory Physiology: the Auditory System VII* (eds Keidel WD, Neff WD), pp. 39–110. New York: Springer.

Hopson JA (1966) The origin of the mammalian middle ear. *Am Zool* **6**, 437–450.

Hou S-L, Meng J (2014) A new eutriconodont mammal from the early Cretaceous Jehol Biota of Liaoning, China. *Chin Sci Bull* **59**, 546–553.

Hurum JH (1998) The inner ear of two Late Cretaceous multituberculate mammals, and its implications for multituberculate hearing. *J Mamm Evol* **5**, 65–93.

Hurum JH, Presley R, Kielan-Jaworowska Z (1996) The middle ear in multituberculate mammals. *Acta Palaeontol Pol* **41**, 253–275.

Huttenlocker AK, Grossnickle DM, Kirkland JI, et al. (2018) Late-surviving stem mammal links the lowermost Cretaceous of North America and Gondwana. *Nature* **558**, 108–112.

Inuzuka N, Hasegawa Y, Nogariya H, et al. (1975) On the stylohyoid bone of Naumann's elephant (Elephas naumanni Makiyama) from Lake Nojiri. *Memoirs of the Faculty of Science, Kyoto University, Ser. Geol. Mineral*. **XLI**, 49–65

Ji Q, Luo Z-X, Zhang X-L, et al. (2009) Evolutionary development of the middle ear in Mesozoic therian mammals. *Science* **326**, 278–281.

Kemp TS (1982) *Mammal-like Reptiles and the Origin of Mammals*. London: Academic Press.

Kemp TS (2007) Acoustic transformer function of the postdentary bones and quadrate of a nonmammalian cynodont. *J Vertebr Paleontol* **27**, 431–441.

Kermack DM, Kermack KA (1984) *The Evolution of Mammalian Characters*. London: Croom-Helm.

Kermack KA, Mussett F, Rigney HW (1973) The lower jaw of Morganucodon. *Zool J Linn Soc* **53**, 87–175.

Kermack KA, Mussett F, Rigney HW (1981) The skull of Morganucodon. *Zool J Linn Soc* **71**, 1–158.

Kielan-Jaworowska Z, Cifelli RL, Luo ZX (2004) *Mammals from the Age of Dinosaurs: Origins, Evolutions, and Structure*. New York: Columbia University Press.

Krause DW, Hoffmann S, Wible JR, et al. (2014) First cranial remains of a gondwanatherian mammal reveal remarkable mosaicism. *Nature* **515**, 512–517.

Lillegraven JA, Krusat G (1991) Cranio-mandibular anatomy of Haldanodon exspectatus (Docodonta; Mammalia) from the Late Jurassic of Portugal and its implications to the evolution of mammalian characters. *Contrib Geol Univ Wyoming* **28**, 39–138.

Luo Z-X (2011) Developmental patterns in Mesozoic evolution of mammal ears. *Annu Rev Ecol Evol Syst* **42**, 355–380.

Luo Z-X, Ketten DR (1991) CT scanning and computerized reconstructions of the inner ear of multituberculate mammals. *J Vertebr Paleontol* **11**, 220–228.

Luo Z-X, Schultz JA, Ekdale EG (2016) Evolution of the middle and inner ears of mammaliaforms: the approach to mammals. In *Evolution of the Vertebrate Ear* (eds Clack JA, Fay RR, Popper AN), pp. 139–174. New York: Springer.

Luo Z-X, Wible JR (2005) A late Jurassic digging mammal and early mammalian diversification. *Science* **308**, 103–107.

Luo Z-X, Crompton AW, Sun A-L (2001) A new mammaliaform from the Early Jurassic and evolution of mammalian characteristics. *Science* **292**, 1535–1540.

Luo Z-X, Kielan-Jaworowska Z, Cifelli RL (2002) In quest for a phylogeny of Mesozoic mammals. *Acta Palaeontol Pol* **47**, 1–78.

Luo Z-X, Chen P, Li G, et al. (2007a) A new eutriconodont mammal and evolutionary development in early mammals. *Nature* **446**, 288–293.

Luo Z-X, Ji Q, Yuan C-X (2007b) Convergent dental adaptations in pseudo-tribosphenic and tribosphenic mammals. *Nature* **450**, 93–97.

Luo Z-X, Yuan C-X, Meng Q-J, et al. (2011) A Jurassic eutherian mammal and divergence of marsupials and placentals. *Nature* **476**, 442–445.

Luo Z-X, Gatesy SM, Jenkins FA, et al. (2015) Mandibular and dental characteristics of Late Triassic mammaliaform *Haramiyavia* and their ramifications for basal mammal evolution. *Proc Natl Acad Sci USA* **112**, E7101–E7109.

Luo Z-X, Meng Q-J, Grossnickle DM, et al. (2017) New evidence for mammaliaform ear evolution and feeding adaptation in a Jurassic ecosystem. *Nature* **548**, 326–329.

Maier W (1990) Phylogeny and ontogeny of mammalian middle ear structures. *Netherlands J Zool* **40**, 55–74.

Maier W, Ruf I (2016) Evolution of the mammalian middle ear: a historical review. *J Anat* **228**, 270–283.

Mallo M (2001) Formation of the middle ear: recent progress on the developmental and molecular mechanisms. *Dev Biol* **231**, 410–419.

Manley GA, Sienknecht UJ (2013) The evolution and development of middle ears in land vertebrates. In: *The Middle Ear* (eds Puria S, Fay RR, Popper AN), pp. 7–30. New York: Springer.

Mao F-Y, Meng J (2019a) A new haramiyidan mammal from the Jurassic Yanliao Biota and comparisons with other haramiyidans. *Zool J Linn Soc* **186**, 529–552.

Mao F-Y, Meng J (2019b) Tooth microwear and occlusal modes of euharamiyidans from the Jurassic Yanliao Biota reveal mosaic tooth evolution in Mesozoic allotherian mammals. *Palaeontology* **62**, 639–660.

Mao F-Y, Zheng X-T, Wang X-L, et al. (2019) Evidence of diphyodonty and heterochrony for dental development in euharamiyidan mammals from Jurassic Yanliao Biota. *Vertebrata PalAsiatica* **57**, 51–76. https://doi.org/10.19615/j.cnki.1000-3118.180803

McClain JA (1939) The development of the auditory ossicles of the opossum (Didelphys virginiana). *J Morphol* **64**, 211–265.

Meng J (1992) The stapes of *Lambdopsalis bulla* (Multituberculata) and transformational analyses on some stapedial features in Mammaliaformes. *J Vertebr Paleontol* **12**, 459–471.

Meng J, Fox RC (1995a) Therian petrosals from the Oldman and milk river formations (Late Cretaceous), Alberta, Canada. *J Vertebr Paleontol* **15**, 122–130.

Meng J, Fox RC (1995b) Osseous inner ear structures and hearing in early marsupials and placentals. *Zool J Linn Soc* **115**, 47–71.

Meng J, Hou S-L (2016) Earliest known mammalian stapes from an early cretaceous eutriconodontan mammal and implications for evolution of mammalian middle ear. *Palaeontologia Polonica* **67**, 181–196.

Meng J, Wyss AR (1995) Monotreme affinities and low-frequency hearing suggested by multituberculate ear. *Nature* **377**, 141–144.

Meng J, Hu Y-M, Wang Y-Q, et al. (2003) The ossified Meckel's cartilage and internal groove in Mesozoic mammaliaforms: implications to origin of the definitive mammalian middle ear. *Zool J Linn Soc* **138**, 431–448.

Meng J, Wang Y-Q, Li C-K (2011) Transitional mammalian middle ear from a new Cretaceous Jehol eutriconodont. *Nature* **472**, 181–185.

Meng J, Bi S-D, Wang Y-Q, et al. (2014) Dental and mandibular morphologies of *Arboroharamiya* (Haramiyida, Mammalia): a comparison with other haramiyidans and Megaconus and implications for mammalian evolution. *PLoS ONE* **9**, e113847.

Meng Q-J, Grossnickle DM, Liu D, et al. (2017) New gliding mammaliaforms from the Jurassic. *Nature* **548**, 291–296.

Meng J, Bi S-D, Zheng X-T, et al. (2018) Ear ossicle morphology of the Jurassic euharamiyidan *Arboroharamiya* and evolution of mammalian middle ear. *J Morphol* **279**, 441–457.

Miao D-S, Lillegraven JA (1986) Discovery of three ear ossicles in a multituberculate mammal. *Natl Geogr Res* **2**, 500–507.

Novacek MJ (1993) Patterns of diversity in the mammalian skull. In: *The Skull*, vol. **2** (eds Hanken J, Hall B), pp. 438–545. Chicago: University of Chicago Press.

Novacek MJ, Wyss A (1986) Origin and transformation of the mammalian stapes. *Contrib Geol Univ Wyoming* **24**, 35–53.

Olson EC (1944) *Origin of mammals based upon cranial morphology of the therapsid suborders. Geol Soc Am* Spec Papers **55**, 1–136.

Palmer RW (1913) Note on the lower jaw and ear ossicles of foetal Perameles. *Anat Anz* **43**, 510–515.

Panciroli E, Schultz JA, Luo ZX (2019) Morphology of the petrosal and stapes of *Borealestes* (Mammaliaformes, Docodonta) from the Middle Jurassic of Skye, Scotland. *Pap Palaeontol* **5**, 139–156.

Parrington FR (1979) The evolution of the mammalian middle and outer ears: a personal review. *Biol Reviews* **54**, 369–387.

Pérez LM, Toledo N, De Iuliis G, et al. (2010) Morphology and function of the hyoid apparatus of fossil xenarthrans (Mammalia). *J Morphol* **271**, 1119–1133.

Presley R (1984) Lizards, mammals and the primitive tetrapod tympanic membrane. *Symp Zool Soc London* **52**, 127–152.

Reichert K (1837) Über die visceralbogen der wirbelthiere im allgemeinen und deren metamorphosen bei den Vögeln und Säugethieren. *Arch Anat Physiol Wissenschaftliche Med* **1837**, 120–220.

Rodrigues PG, Ruf I, Schultz CL (2013) Digital reconstruction of the otic region and inner ear of the non-mammalian cynodont *Brasilitherium riograndensis* (Late Triassic, Brazil) and

its relevance to the evolution of the mammalian ear. *J Mammal Evol* **20**, 291–307.

Rougier GW, Wible JR, Novacek MJ (1996) Middle-ear ossicles of the multituberculate *Kryptobaatar* from the Mongolian Late Cretaceous: implications for mammaliamorph relationships and the evolution of the auditory apparatus. *Am Mus Novitates* **3187**, 1–43.

Rowe T (1996) Coevolution of the mammalian middle ear and neocortex. *Science* **273**, 651–654.

Rowe T, Rich TH, Vickers-Rich P, et al. (2008) The oldest platypus and its bearing on divergence timing of the platypus and echidna clades. *Proc Natl Acad Sci USA* **105**, 1238–1242.

Ruf I, Luo Z-X, Wible JR, et al. (2009) Petrosal anatomy and inner ear structures of the Late Jurassic *Henkelotherium* (Mammalia, Cladotheria, Dryolestoidea): insight into the early evolution of the ear region in cladotherian mammals. *J Anat* **214**, 679–693.

Ruf I, Luo Z-X, Martin T (2013) Reinvestigation of the basicranium of *Haldanodon exspectatus* (Mammaliaformes, Docodonta). *J Vertebr Paleontol* **33**, 382–400.

Sánchez-Villagra MR, Gemballa S, Nummela S, et al. (2002) Ontogenetic and phylogenetic transformations of the ear ossicles in marsupial mammals. *J Morphol* **251**, 219–238.

Schultz JA, Ruf I, Martin T (2018) Oldest known multituberculate stapes suggests an asymmetric bicrural pattern as ancestral for Multituberculata. *Proc Biol Sci* **285**, 20172779.

Segall W (1970) Morphological parallelisms of the bulla and auditory ossicles in some insectivores and marsupials. *Fieldiana Zool* **51**, 169–205.

Shoshani J, Ferretti MP, Lister AM, et al. (2007) Relationships within the Elephantinae using hyoid characters. *Quatern Int* **169**, 174–185.

Sigogneau-Russell D, Frank P, Hemmerlé J (1986) A new family of mammals from the lower part of the French Rhaetic. In: *The Beginning of the Age of Dinosaurs: Faunal Change across the Triassic-Jurassic Boundary* (ed. Padian K), pp. 99–108. Cambridge: Cambridge University Press.

Simmons NB, Seymour KL, Habersetzer J, et al. (2010) Inferring echolocation in ancient bats. *Nature* **466**, E8.

Takada Y, Izumi M, Gotoh K (2009) Comparative anatomy of the hyoid apparatus of carnivores. *Mammal Study* **34**, 213–218.

Takechi M, Kuratani S (2010) History of studies on mammalian middle ear evolution: a comparative morphological and developmental biology perspective. *J Exp Zool B Mol Dev Evol* **314B**, 1–17.

Van Kampen PN (1905) Die Tympanalgegend des Säugetierschädels. *Gegenbaurs Morphol Jahrb* **34**, 321–722.

Vater M, Meng J, Fox RC (2004) Hearing organ evolution and specialization: early and later mammals. In *Evolution of the Vertebrate Auditory System* (eds Manley GA, Popper AN, Fay RR), pp. 256–288. New York: Springer.

Veselka N, McErlain DD, Holdsworth DW, et al. (2010) A bony connection signals laryngeal echolocation in bats. *Nature* **463**, 939–942.

Wang Y-Q, Hu Y-M, Meng J, et al. (2001) An ossified Meckel's cartilage in two Cretaceous mammals and origin of the mammalian middle ear. *Science* **294**, 357–361.

Watson D (1953) The evolution of the mammalian ear. *Evolution* **7**, 159–177.

Weissengruber G, Forstenpointner G, Peters G, et al. (2002) Hyoid apparatus and pharynx in the lion (*Panthera leo*), jaguar (*Panthera onca*), tiger (*Panthera tigris*), cheetah (*Acinonyx jubatus*) and domestic cat (*Felis silvestris* f. *catus*). *J Anat* **201**, 195–209.

Wible JR (1991) Origin of Mammalia: the craniodental evidence reexamined. *J Vertebr Paleontol* **11**, 1–28.

Wible JR (2008) On the cranial osteology of the *Hispaniolan solenodon*, *Solenodon paradoxus* Brandt, 1833 (Mammalia, Lipotyphla, Solenodontidae). *Ann Carnegie Mus* **77**, 321–402.

Wible JR (2010) On the hyoid and larynx of the *Hispaniolan solenodon*, *Solenodon paradoxus* Brandt, 1833 (Mammalia, Lipotyphla, Solenodontidae). *Ann Carnegie Mus* **79**, 29–38.

Wible JR, Hopson JA (1993) Basicranial evidence for early mammal phylogeny. In: *Mammal Phylogeny: Mesozoic Differentiation, Multituberculates, Monotremes, Early Therians, and Marsupials* (eds Szalay FS, Novacek MJ, McKenna MC), pp. 45–62. New York: Springer Verlag.

Wible JR, Rougier GW (2000) Cranial anatomy of *Kryptobaatar dashzevegi* (Mammalia, Multituberculata), and its bearing on the evolution of mammalian characters. *Bull Am Mus Nat Hist* **247**, 1–120.

Wible JR, Spaulding M (2012) A reexamination of the *Carnivora malleus* (Mammalia, Placentalia). *PLoS ONE* **7**, e50485.

Zeller U (1989) Die Entwicklung und Morphologie des Schädels von *Ornithorhynchus anatinus* (Mammalia: Prototheria: Monotremata). *Abh Senckenberg Nat Ges* **545**, 1–188.

Zeller U (1993) Ontogenetic evidence for cranial homologies in monotremes and therians, with special reference to Ornithorhynchus. In: *Mammal Phylogeny: Mesozoic Differentiation, Multituberculates, Monotremes, Early Therians, and Marsupials* (eds Szalay FS, Novacek MJ, McKenna MJ), pp. 95–107. New York: Springer.

Zheng X-T, Bi S-D, Wang X-L, et al. (2013) A new arboreal haramiyid shows the diversity of crown mammals in the Jurassic period. *Nature* **500**, 199–202.

Zhou C-F, Wu S-Y, Martin T, et al. (2013) A Jurassic mammaliaform and the earliest mammalian evolutionary adaptations. *Nature* **500**, 163–167.